Benemérita Universidad Autónoma de Puebla

Facultad de Ciencias Físico Matemáticas

DESIGN OF THE FORWARD DIFFRACTIVE DETECTOR'S CONTROL SYSTEM FOR CERN-LHC RUN 3

Tesis

que para obtener el grado de

Doctor en Ciencias (Física Aplicada)

presenta

Saúl Aníbal Rodríguez Ramírez

Asesor: Arturo Fernández Téllez

Asesor: Guillermo Tejeda Muñoz

CERN-THESIS-2023-081
08/06/2023

Puebla, Pue. Junio 2023

COMITÉ

Severino Muñoz Aguirre
PRESIDENTE

Mario Iván Martínez Hernández
SECRETARIO

Mario Rodríguez Cahuantzi
VOCAL

Arturo Fernández Téllez
ASESOR

Guillermo Tejeda Muñoz
ASESOR

Solangel Rojas Torres
VOCAL EXTERNO

Juan Carlos Cabanillas Noris
VOCAL EXTERNO

Germán Ardul Muñoz Hernández
SUPLENTE

DEDICATORIA

Para mis padres, Eloísa y Alberto Saúl. Mamá Elo y Papá Saúl. Ayer, hoy y siempre, para ustedes, por ustedes y gracias a ustedes.

Agradecimientos

Al doctor Arturo Fernandez Téllez, asesor, amigo y mentor. Gracias por su contagioso entusiasmo por la ciencia y el trabajo, gracias por sus ánimos y sus enseñanzas, por su siempre constante apoyo y supervisión.

Al doctor Guillermo Tejeda Muñoz, también asesor, amigo y mentor desde hace ya varios años. Gracias por sus invaluables enseñanzas, su guía certera y su ejemplo a seguir.

A Juan Manuel Mejía Camacho, co-autor del artículo publicado sobre este trabajo y quien cimentó las bases del DCS de FDD. Gracias por todo el trabajo compartido, por el apoyo y la retroalimentación.

A Solangel Rojas Torres, responsable de FDD, amigo y mentor en los años que pasé en el CERN. Gracias por estar siempre al pie del cañón, y sobre todo por tu disposición a apoyar y asesorar.

A los doctores Mario Iván Martínez Hernández y Juan Carlos Cabanillas Noris, miembros de mi jurado y en la práctica un par de asesores más. Gracias por toda su paciencia y sus valiosísimas enseñanzas al introducirme en el área de sistemas de control.

Al resto de miembros de mi jurado: doctores Mario Rodríguez Cahuantzi, Severino Muñoz Aguirre y Germán Ardul Muñoz Hernández, por su invaluable retroalimentación a lo largo de mi doctorado.

A todos los colegas del grupo FIT, especialmente a: Vojtech Zabloudil (compañero en la construcción de FDD), Maciej Slupecki (coordinador general de FIT), Jacek Otwinowski (miembro de FV0 y responsable del trigger de FIT), Wladyslaw Trzaska (líder y portavoz del grupo FIT), Nikita Vozniuk (desarrollador del Control Server), Mikhail Sukhanov (desarrollador de FT0 DCS), y a todos los demás que de una u otra forma contribuyeron a este trabajo o me apoyaron de diversas formas: Varlen Grabski, Andreas Molander, Dmitry Serebryakov, Dmitry Finogeev, Kristian Gulbrandsen, Arvind Kuntia, Tatiana Karavicheva, Artur Furs, Kristian Roslon, Monika Kutyla, Ildefonso León, y los que me faltaron por nombrar.

Gracias al CONACYT por las becas de doctorado y de movilidad que me otorgaron, y sin las cuales la realización de este trabajo habría sido imposible.

Gracias a Jan Buytaert y Paula Collins por acogerme en el proyecto del High Energy Ventilator y por toda la guía que me brindaron.

Gratitud eterna a los amigos y seres queridos que me acompañaron, me apoyaron o convivieron conmigo de una u otra forma durante este largo proceso, especialmente a Luis y Raúl, quienes fueron guías para mí en un mundo desconocido, pero también a Óscar, Alicia, Jimena y Mario por su incondicional apoyo y amistad. A Sergio, Tonatiuh, Emigdio y David por tantas vivencias y trabajo compartido. A Alejandra, por tantas cosas, por tu fe en mí y tu cariño. Cada uno de ustedes sabe lo mucho que le debo. Gracias por su apoyo, su cariño y su compañía, algunos estando cerca y otros al otro lado del mundo. Gracias especiales a la maestra Eva Medel Báez, mi ex-asesora, por su amistad y su confianza a lo largo de todos estos años.

No me alcanzarían las palabras para agradecer todo lo que le debo a mi amada familia, especialmente a mis hermanos Ney, Dama y Narda. Sin ustedes no habría podido hacer absolutamente nada. Gracias por sus enseñanzas, por ser otros padres y madres para mí, por recibirme siempre en sus hogares (especialmente Dama), y por mil cosas más. A mis queridísimos sobrinos: Dania, Lesly, Jorge, Armando, Tere, Narda, Paloma y Ameyali, por tantas vivencias, juegos, películas y por ser los hermanos pequeños que no tuve. Gracias también a mis cuñados Armando, Miroslava y Óscar, a mis tíos y a mis primos. Gracias por su amor, su inquebrantable fe en mi, su incondicional apoyo, y por tantas cosas que me sería imposible terminar de nombrar.

Pero como siempre y principalmente gracias a mis padres, quienes son el motor de mi vida. Esta tesis es para ustedes.

Gracias a Dios por todo.

Abstract

The ALICE experiment is currently participating in the recently started Run 3 of CERN LHC, in which collision rate and thus data stream rate had been significantly increased with respect to Run 2. Several upgrades were required for ALICE prior to the start or Run 3, including implementation of a new Online-Offline (O2) system to handle the new data flow, and upgrading detectors. For instance, the AD (ALICE Diffractive) was replaced by the new Forward Diffractive Detector (FDD) and included in the Fast Interaction Trigger (FIT) project. Therefore, development of a Detector Control System (DCS) for FDD was necessary. The DCS is one of the fundamental systems of CERN experiments which allows for essential tasks such as remote and safe operation, monitoring, configuration and recording of data. The aim of this work was to collaborate in the design, development and integration of the DCS for FDD, as well as taking part of installation and calibration of the detector. Specific objectives also include communicating the DCS to its corresponding experimental equipment, implementing the FDD-DCS according to the general requirements of the FIT project and the particular ones for FDD, integrating the DCS to the ALICE central DCS observing all of its guidelines, and optimizing the configuration process of FDD through the DCS for data taking. Chapter 1 briefly defines ALICE, FIT, FDD and their main purpose. Chapter 2 describes the components of a DCS, emphasizing the software tools required for its development. Chapter 3 lists the hardware equipment to be controlled by the DCS. Chapter 4 describes the modeling of FDD-DCS as a hierarchical structure composed of finite state machines and explains the design of the various user interface panels for operators. Chapter 5 describes configuration of several DCS features essential for operation: the alarm, archiving and SAFE systems, the trending panels and the automated configuration process. A manuscript based on this work was accepted and published in the Nuclear Instruments and Methods in Physics Research A scientific journal.

Contents

List of Figures

List of Tables

Chapter 1

Introduction

1.1 The ALICE experiment at CERN LHC

The European Organization for Nuclear Research (CERN) is an international organization consisting of 22 member states with headquarters in Geneva, Switzerland, dedicated to the study of Particle Physics. CERN's Large Hadron Collider (LHC) is a circular, 27 km diameter particle accelerator (the largest in the world) installed underground (from 45 m to 170 m below the surface) in the region across the border between France and Switzerland. LHC consists of two parallel rings with four intersection points. High-energy particle beams are injected in the rings and accelerated in opposite directions until they collide on the interaction points. The four great CERN experiments are built around those points[1].

ALICE (A Large Hadron Collider Experiment) is a heavy-ion detector experimental system located at LHC interaction point number 2, with overall dimensions of $16 \times 16 \times 26$ m^3 and a total weight of around 10,000 tons. Its main purpose is the study of quantum chromodynamics (QCD), the strong interaction sector of the Standard Model of particle physics[2]. More specifically, ALICE aims to study the non-perturbative part of the QCD, that is, the physics of the quark-gluon plasma (QGP) at high energy densities and temperatures.

ALICE is composed of several subdetectors using different particle detection techniques that can be grouped as follows[2][3]:

- Tracking detectors, extracting particle momentum and charge.
- Calorimeters, providing energy of selected particle species.
- Time of flight, reconstructing particle masses and contributing to particle identification.

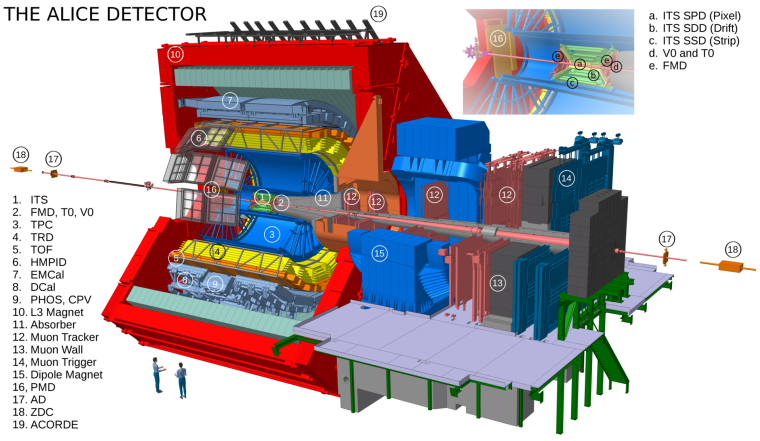

Figure 1.1: Overview of the ALICE experiment at CERN LHC during run 2.

- Transition radiation detector, measuring particle momenta and also participating in particle identification.
- Muon arm, focusing on properties of highly-penetrating muons.
- Forward and trigger detectors, detecting global collision properties independently from the others.

ALICE has operated during LHC Run 1 (2009-2013) and Run 2 (2015-2018). Figure 1.1 shows the ALICE experiment configuration during the latter. Run 3 started in 2022, after LHC second Long Shutdown (LS2). The upgrades that LHC went through in LS2 required in turn a major upgrade or replacement of multiple subdetectors in ALICE.

1.1.1 The Standard Model

The Standard Model (SM) of Physics is a theory that describes the most elementary particles of nature and the way they interact with each other. Though incomplete, it is right now the theory that better explains the behaviour of quantum particles.

As shown in Figure 1.2, particles in the SM are divided in fermions (subsequently divided in quarks and leptons) and bosons. These particles interact via three of the four fundamental forces (or interactions) of nature: electromagnetism, strong force and weak force, being the absence of gravity its major shortcoming (however, quantum gravity is extremely weak compared to the other interactions

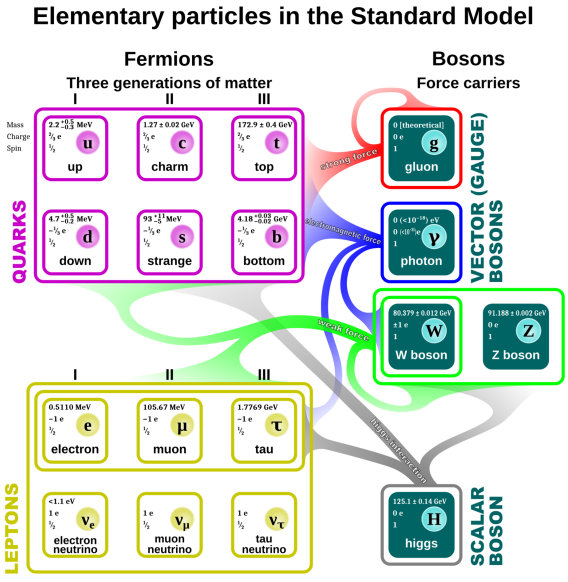

Figure 1.2: Diagram of the Standard Model of particle physics[3].

and can be neglected). For each interaction there's a gauge boson or force carrier: the photon carries the electromagnetic interaction; W+, W- and Z bosons carry the weak interaction; and gluons carry the strong interaction. There's also a scalar boson, named the Higgs boson, responsible for the existence of mass. Experimental confirmation of the Higgs boson existence, performed at CERN in 2012, was a major experimental discovery for Physics.

1.1.2 The quark-gluon plasma

The quark-gluon plasma is a state of matter in which, unlike normal matter, quarks and gluons are not confined. It could be described as an extremely hot and dense fluid, the hottest and densest ever produced in a laboratory. It is speculated that the early Universe existed in such a state around 10^{-6} seconds after the Big Bang, and its properties affected the development of the Universe. For instance, quantum fluctuations (believed to have appeared in that period) could have been responsible for the structure formation process of the early Universe, generating galaxies and clusters[3]. ALICE was specifically designed to study the QGP created at LHC energies[4].

Quantum Chromodynamics is a part of the SM that describes the strong in-

teraction of matter. According to QCD, quarks and gluons are the elementary particles carrying the "charge" of the strong interaction, known as colour. There are three colours: red, green, blue and their anticolours. Particles can exist only if they are colour neutral, a phenomenon also known as colour confinement. Colour neutrality is achieved by a combination of all of the three colours at once or by a combination of a colour with its corresponding anticolour. Quarks have a net colour and cannot exist by themselves, so they combine to produce neutral colour particles, known as hadrons. Quarks inside hadrons are held together by gluons, i.e. the strong force interaction. Hadrons are divided according to their number of quarks in mesons (two quarks) and baryons (three quarks). Among baryons there are the components of the atomic nuclei: protons and neutrons.

Another important property of QCD is the asymptotic freedom, which formulates that the interaction between particles becomes asymptotically weaker as the energy increases and the distance decreases.

In the QGP, colour confinement is no longer present, meaning that quarks and gluons can exist by themselves, and due to asymptotic freedom they behave as almost free particles since conditions of high energy and short distances are met. The QGP can be produced heating a many body system of quarks and gluons under the conditions of large energy density to a temperature exceeding 150-160 MeV (equivalent to more than 10^{12} K).

High-energy nuclear collisions in the TeV energy range at the LHC provide the required temperature and density conditions to produce a long-lived QGP. A thorough characterization of the QGP state and its related phenomenology is the subject of the ALICE experimental program and has inspired the design of its detector. Additionally, thanks to its high precision tracking and excellent particle identification, ALICE has contributed to addressing further fundamental aspects of the strong interaction and QCD, such as studying the production of light antinuclei and hyper-nuclei, the kaon-nucleon and the hyperon-nucleon interaction, which gives us insights on the manifestations of hadronic interactions. Such studies can be efficiently performed in ALICE, either with Pb–Pb or high-multiplicity pp collisions. ALICE has also contributed to the study of specific QCD processes in pp collisions like measurement of inclusive and heavy-flavour jet production and studies of open heavy flavour, quarkonia and high-pT hadrons. ALICE's main topics of investigation can be summarized in the following physics questions:[4]

- What are the thermodynamic, hydrodynamic and transport properties of the QGP produced at the LHC?
- How does the QGP affect the formation of hadrons and the propagation of energetic partons?
- How does deconfinement in the QGP affect the QCD force?

- Can the QGP lead to discovery of novel QCD effects?
- What are the limits of QGP formation?
- What is the nature of the initial state of heavy-ion collisions?
- What is the nature of hadron-hadron interactions?
- Can ALICE elucidate specific aspects of perturbative QCD and of related "long distance" QCD interactions?

1.2 Particle physics parameters

Currently, only tiny and short-lived samples of QGP can be produced in laboratory since they quickly expand, lose the required energy density and revert into hadronic matter. High-energy particle collisions is the only known method to generate a QGP artificially, and heavy-ion collisions are preferable over light ions or protons in order to create the largest possible sample.

In heavy-ion collisions, the number of experimental observables is very limited. At best the yields of identified particles as a function of the transverse momentum, the azimuth angle and the pseudorapidity are available. These observables can be used to calculate the luminosity, which is needed for the determination of cross sections. Invariant mass distributions may also be derived. Some of these parameters are described in this section.

1.2.1 Impact parameter and centrality

The impact parameter b is the perpendicular distance between the path of a projectile and the centre of the target. In high-energy nuclear physics, collisions may be classified according to their impact parameter. Central collisions have $b \approx 0$, peripheral collisions have $0 < b < 2R$, and ultraperipheral collisions (UPCs) have $b > 2R$, where the colliding nuclei are viewed as hard spheres with radius R.

Centrality describes how central a given event is when compared to other events in the same sample. Events are divided into centrality classes, where the centrality class of 0-10% means 10% of most central events, while most peripheral events are assigned the centrality of 80-100%. The centrality is one of the most important parameters describing a collision, because it is related to the amount of energy available for physics processes and therefore forms a basis allowing to compare the measurements between different experiments, using different beam energies and collision systems.

1.2.2 Cross section

The cross section σ is a fundamental concept in particle physics. It represents the probability of a specific process will take place. The differential cross section, defined as $\frac{d\sigma}{d\Omega}$, states the probability of producing a scattered particle per solid angle. The total cross section σ_{tot} is obtained by integrating the differential cross section over the full solid angle:

$$\sigma_{tot} = \oint \frac{d\sigma}{d\Omega} d\Omega = \int_0^{2\pi} \int_0^{\pi} \frac{d\sigma}{d\Omega} sin\theta d\theta d\varphi \tag{1.1}$$

1.2.3 Luminosity

In particle physics experiments the energy available for the production of new effects is a very important parameter. The required large centre of mass energy can only be provided with colliding beams where little or no energy is lost in the motion of the centre of mass system (cms). Besides the energy the number of useful interactions (events), is important. This is especially true when rare events with a small production cross section σ_p are studied. The quantity that measures the ability of a particle accelerator to produce the required number of interactions is called the luminosity and is the proportionality factor between the number of events per second dR/dt and the cross section σ_p:

$$\frac{dR}{dt} = L \cdot \sigma_p \tag{1.2}$$

The units of luminosity are therefore $\mathrm{cm}^{-2}\mathrm{s}^{-1}$. The total amount of events detected over a time period of length T is related to the integrated luminosity L_{int}, calculated as:

$$L_{int} = \int_0^T L dt \tag{1.3}$$

where the number of events of interest R is:

$$L_{int} \cdot \sigma_p = R \tag{1.4}$$

The units for integrated luminosity are usually expressed as b^{-1} where $\mathrm{b}=10^{-28}\mathrm{m}^2$.

1.2.4 Pseudorapidity

The pseudorapidity (η) is a spatial coordinate commonly used in the experimental particle physics. It only depends on the angle (θ) of particle's momentum with respect to the beam axis and is defined as:

$$\eta = -ln[tan(\theta/2)] \tag{1.5}$$

Since pseudorapidity describes the angle of a particle outgoing from the collision region it is a convenient parameter to describe a detector's coverage. Detector located at mid-rapidity, i.e., ($-1 \leq \eta \leq 1$) will be exposed to different particle fluxes than a forward-rapidity detector, ($-2 \geq \eta \geq 2$), located close to the beam pipe or farther from the collision region along the beam axis. Furthermore, the available range of physics processes changes with rapidity.

In a collider experiment pseudorapidity, together with azimuth angle (ϕ) and transverse momentum denoted as pT, i.e., momentum perpendicular to the beam axis, are commonly used to describe properties of detected particles.

1.3 The ALICE upgrade program

For LHC Run 3, the targeted integrated luminosity is 13 nb^{-1} in Pb–Pb collisions, meaning that the collision rates will increase by a factor of 100 with respect to Run 2, up to 50 kHz, which implies approximately 3.5 TB/s of data. In order to both adapt and exploit these new conditions, ALICE went through major upgrades during the LS2. The upgraded ALICE will focus on rare, complex probes at low transverse momentum, which led to improvements in vertexing and tracking resolution. High statistics and high precision measurements are required, which will give access to the rare physics channels needed to understand the dynamics of the condensed phase of QCD.

The ALICE upgrades for Run 3 can be summarized in the following[3]:

- Readout upgrade
- New Inner Tracking System
- New Muon Forward Tracker
- New readout chambers for the TPC
- Integrated Online-Offline (O^2) system (see section 1.3.1).
- New Fast Interaction Trigger (FIT) (see section 1.3.2).

1.3.1 Online-Offline (O^2) system

In order to cope with the new requirements for Run 3, and based on the experience accumulated in design and operation of the online and offline systems during Run 1 and Run 2, the new Online-Offline (O^2) computing system for ALICE was developed[5].

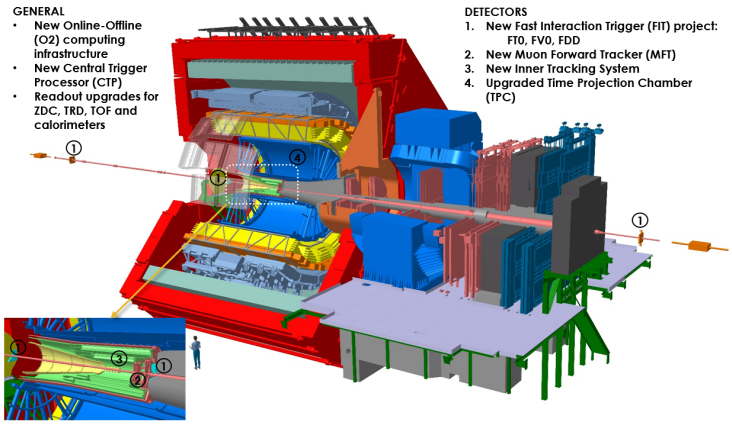

Figure 1.3: ALICE upgrades for Run 3.

For LHC Runs 1 and 2, the ALICE experiment had five Online systems: Trigger, Data Acquisition (DAQ, in charge of the data-flow from the detector up to the data storage, as well as performing the data quality monitoring and the system performance monitoring), High-Level Trigger (HLT, in charge of reducing the volume of physics data by selection and compression of the data), Detector Control System (DCS, described in section 2) and Experiment Control System (ECS, in charge of coordinating the activities of all the online systems to fulfil their common goal). On the other hand there was the Offline systems for calibration, simulation, reconstruction and analysis tasks. O^2 is the replacement of the DAQ, HLT, and Offline systems. As such, O^2 will implement a distributed, parallel and staged data processing model. It is designed to combine all the computing functionalities needed in a high energy physics experiment: detector read-out, event building, data recording, detector calibration, data reconstruction, physics simulation and analysis. It can also be adapted to different configurations according to the detectors' specific needs.

O^2 is characterized by a continuous readout mode with simultaneous data processing, data compression by means of partial online reconstruction and calibration, and the sharing of common computing resources during and after data taking.

The data flow in the O^2 system is shown in Figure 1.4. The First Level Processors (FLPs) and the Event Processing Nodes (EPNs) are the new computing devices for data collection and data volume reduction. FLPs read the raw data from the detectors' readout electronics and reduce their volume by splitting them into physics and slow control data. Physics data is transferred from the FLPs

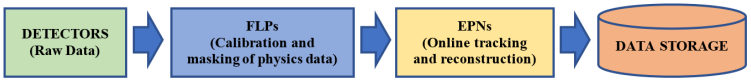

Figure 1.4: Diagram of the O^2 data flow.

to the EPNs at a rate of 500 GB/s. EPNs process the raw data online while performing reconstruction tasks. Only reconstructed data is transferred to the storage, while the raw data is discarded.

Global reconstruction and events extraction is performed asynchronously in iterative passes, either on the EPNs, or on the Grid to offload processing. Calibration is integrated at different processing stages on the FLPs and EPNs, both to minimise data transport and to make results available as early as possible in the chain; this is the key to real-time data reduction. The Condition and Calibration Data Base (CCDB) is populated and used at all stages, synchronously and asynchronously. The global data flow also includes data sampling at all levels, in order to feed the Quality Control (QC) system as needed; the results will be stored in a dedicated database.

1.3.2 The Fast Interaction Trigger

Although the ALICE upgrade aimed to set a continuous readout mode to cope with the new data rate for Run 3, not all of ALICE subdetectors could be adequately upgraded to follow this scheme. Consequently, a fast trigger detector was necessary to provide an external trigger or a wakeup signal for the operation of several subdetectors. The rest of them may utilize these triggers, even if it s not technnically required for their operation, with the only exception of TPC.

An external trigger was, therefore, either necessary or at least useful for the majority of ALICE detectors. The need for such a set of triggers is the main motivation to add the FIT system[3].

ALICE triggers system

The Central Trigger Processor (CTP) handles the triggers in ALICE. The CTP collects trigger signals from many detectors and systems and processes them to form the triggers accepted by the Local Trigger Units (LTUs) and forwarded to the Common Readout Units (CRUs), which manage data flow to the O^2 system.

Table 1.1 lists the trigger requirements for ALICE detectors. LM stands for Level Minus One, L0 for Level Zero and L1 for Level One. The latencies associated with these trigger levels are 425 ns, 1200 ns and 6100 ns, respectively. By default,

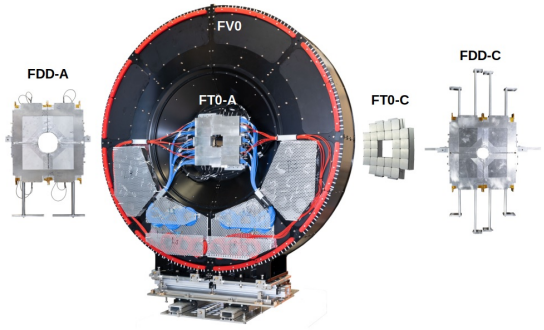

Figure 1.5: FIT components. Side-by-side, in-scale photographs of FIT components. The diameter of the largest element (FV0) is 1.5 m.

all detectors expect a minimum-bias trigger, and some of them an additional multiplicity-based trigger. FIT aims to contribute with both.

Detector	Trigger Level	Trigger Type	Trigger essential
TRD	LM	Minimum Bias	Yes
CPV	LM	Minimum Bias, Multiplicity	Yes
HMPID	LM	Minimum Bias, Multiplicity	Yes
EMCAL	L0	Minimum Bias, Multiplicity	Yes
PHOS	L0	Minimum Bias, Multiplicity	Yes
ITS	LM	Minimum Bias	No
MFT	LM	Minimum Bias	No
ZDC	L0	Minimum Bias	No
TOF	L1	Minimum Bias	No
MCH	L1	Minimum Bias	No
MID	L1	Minimum Bias	No
TPC	-	-	No

Table 1.1: Trigger requirements of ALICE detectors for Run 3.

FIT layout

FIT consists of three subsystems: FT0, FV0 and FDD (see Figure 1.5), each one optimized for different function and operational regime: FT0 is a 208 pixel Cherenkov detector array with good time resolution that plays a major role in trigger generation as well as calculations of collision time and vertex position. FV0 is a large scintillator ring with 48 channels that improves trigger efficiency and dynamic range, also suitable for background monitoring. FDD, described in detail in the next section, covers the pseudorapidity region and is esential for tagging diffractive events and background monitoring.

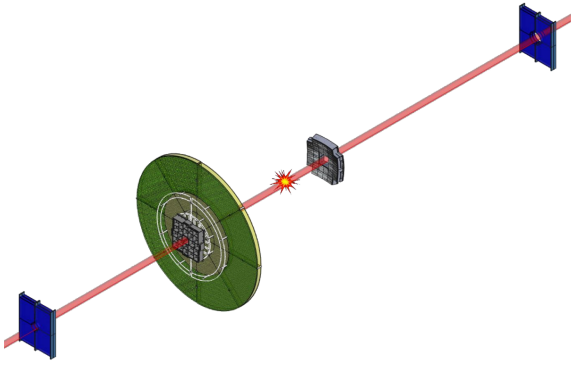

Figure 1.6: Scheme of the FIT detector along the beamline (distances not up to scale). From bottom left: FDD-A (blue), FT0-A (grey), FV0 (green), interaction point, FT0-C (grey) and FDD-C (blue).

1.4 The Forward Diffractive Detector

The Forward Diffractive Detector (FDD)[6][7] is the upgrade for LHC Run 3 of the ALICE Diffractive (AD) detector that took part in Run 2[8]. FDD consists of two stations: FDD-A and FDD-C, located in sides A and C of the ALICE cavern at distances of 17 and 19.5 meters from the interaction point (IP) along the beamline, respectively (see Figure 1.6).

Both stations are composed of two layers, each one made up of four plastic scintillator modules located around the beam pipe, for a total of 16 modules and thus 16 readout channels. The A and C side modules differ only in their inner corner due to the difference in the beam pipe radius on their corresponding sides. Every module is coupled to a pair of wavelength shifting (WLS) bars that collect the light produced by the plastic scintillators. This light is further trasmitted to photomultiplier tubes (PMTs) via bundles of 192 optical fibers (96 for each WLS bar). PMTs send the resulting electrical signal to the FDD FEE. Figure 1.7 A) shows the scheme of a FDD station with all its components.

Each plastic scintillator module is covered in 3 layers of wrapping, the first two for reflective purposes and the last one for protective purpose. The reflective layers provide proper light insulation blocking incoming external light into the module. Aditionally, each station is mounted on an aluminum frame to hold and give stability to the modules and fiber bundles, which is particularly important given the fragility of the fibers. Figure 1.7 B) shows the assembled FDD-C array, including the frame with fiber holders.

The main purpose of FDD is to enhance the ALICE pseudorapidity coverage

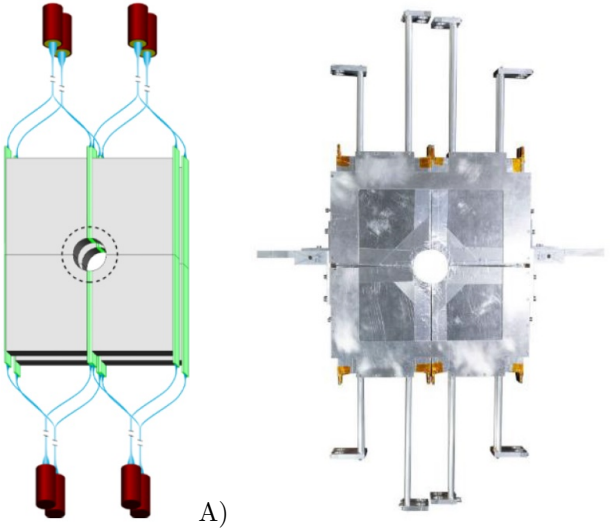

Figure 1.7: A) Scheme of FDD-C station. WLS bars are depicted in green, fiber bundles in blue and PMTs in red. The black dashed line indicates the bigger beam pipe radius at the location of FDD-A. B) FDD-C modules mounted on its aluminum frame before installation. The rods with clamps extending from the top and bottom of FDD support the fragile fiber bundles.

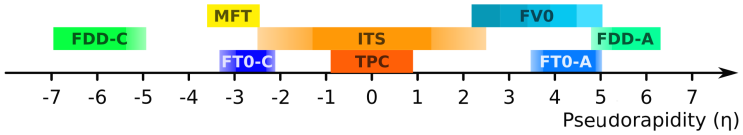

Figure 1.8: Pseudorapidity coverage of selected ALICE subdetectors compared to the FIT project

for the study of diffractive and ultraperipheral events, playing an important role in tagging photon-induced processes. Moreover, FDD will allows us to extend our understanding of diffraction by studying it at higher collision energies of 14 TeV, available only after the LS2. Figure 1.8 shows the pseudorapidity range for selected ALICE detectors. As seen, FDD covers the pseudorapidity ranges of $4.7 \leq \eta \leq 6.3$ and $-6.9 \leq \eta \leq -4.9$, respectively, being the only detector to cover such region.

FDD will also participate in the multiplicity and centrality estimation, complementing the other FIT detectors and the Zero-Degree Calorimeter (ZDC). Its contribution is important especially on the C side, where FV0 is missing. It will also serve as auxiliary luminometer and beam quality monitor by tagging the beam-gas interactions.

The main changes for FDD with respect to AD are:

- Upgrade to a faster state-of-the-art WLS (NOL-38)[9] that decreases light reemission time from 8.5 to 0.95 ns.
- Upgrade to a faster plastic scintillator (BC-420)[10] that matches the absorption wavelength of the WLS bar.
- The use of newly developed Front-End electronics suitable for operation both in a triggered and in a continuous readout mode.
- FDD is equipped with a dedicated laser calibration system that allows for calibration measurements of time and amplitude, quality assurance, and monitoring of the gain and ageing of the detector.

1.4.1 Plastic scintillators

Scintillators are materials with the property of luminescence (i.e. they are able to emit photons) when excited by ionising radiation. This family of materials is covered by both organic and inorganic structures, with some similarities but also with different photophysical processes occurring underneath. Scintillation detectors in conjunction with photomultiplier tubes remain widely used in physics.

Scintillation materials must meet several requirements, including:

- Efficient conversion of kinetic energy into detectable light.
- Linear dependence between the number of photons emitted (light yield) and the deposited energy and number of particles interacting with the scintillator.
- Transparency to its own emission spectrum to prevent reabsorption within the material.
- Short decay time to produce fast signals.
- Emission of light in a wavelength appropriate for the sensor that converts the light into an electrical signal.
- Suitability for cost-effective manufacturing in desired sizes.

Inorganic scintillators are characterized by the good light yield production and linearity, but the time response is relatively slow in comparison with the organics. They are made of crystals whose scintillation effect depends on the change of the state of the valence electrons that are excited when a particle transfers energy to them, and the light is emitted when the electrons return to its base state. The disadvantage of the inorganic scintillators is that they tend to age faster and are more expensive than organic.

The fluorescence process of organic scintillators comes from electronic transitions in the level structure of a a single molecule. Those molecules uses the p-electrons orbital structure, which can be excited from a base energy state S0, as the shown in Figure 1.9, to a higher molecular state S1, S2 or S3, when it absorb the kinetic energy of a charged particle passing nearby. This energy excess is emitted by the particle as a photon and return to S0. The states with excess vibrational energy (such as S11 or S12) are quickly de-excited (on the order of picoseconds) to S10 through radiationless internal conversion. The scintillation light (fluorescence) comes mainly from S1 to the base state. The intensity of the fluorescence at the time t is described in terms of the time decay t of the transition from S10 level according to:

$$I = I_0 s^{-t/\tau} \tag{1.6}$$

where t is around few nanoseconds. The transitions to the T-states are undesirables due that the time transition is longer (on the order of 10^{-3} seconds) than the S-states.

The FDD subdetector needs to be fast enough to avoid overlapping signals from consecutive bunch crossings from the LHC. Consequently, plastic organic scintillators were selected for FDD, as they provide the needed speed at a reasonable cost.

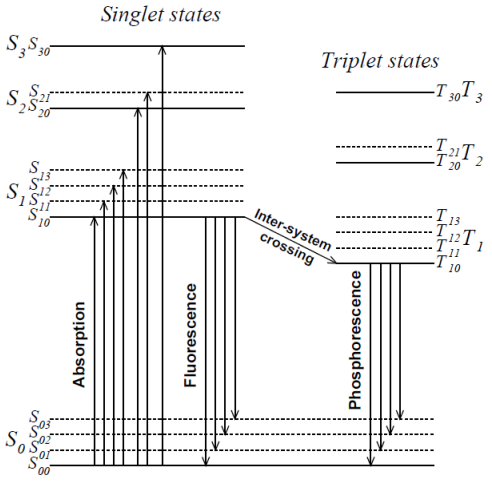

Figure 1.9: Energy levels of an organic molecule with π-electron structure.

1.4.2 Ultra-peripheral collisions

Heavy ions moving at relativistic speed are accompanied by strong electromagnetic fields. Since the electric and magnetic fields are perpendicular to each other, combined they may be treated as a flux or nearly-real virtual photons by some approximations. The maximum photon energy depends on the width of the fields in the direction of motion $k_{max} = 2\gamma\hbar c/b$, where γ is the Lorentz boost of the ion, and b is the impact parameter.

Ultra-peripheral collisions are interactions between the electromagnetic field of one ion and another ion (or also its electromagnetic field), in which the impact parameter is larger than the sum of their radii[11].

Vector meson photoproduction is the most intensively studied UPC reaction (and the most relevant for the FDD subdetector). The cross-sections are large and most of the final states are simple. In photoproduction, the incident photon fluctuates to a quark-antiquark pair (forming a colour dipole) which then interacts with a target nucleon and scatters quasi-elastically, emerging as a vector meson. The scattering is mediated by the strong force, but occurs without a net color exchange. The vector meson is further measured via its dileptonic decay.

Chapter 2

Detector Control System Components

2.1 Overview of a DCS

Every detector in ALICE consists of many complex experimental equipment including high voltage sources, electronic boards, among others. Furthermore, ALICE is located 50 meters underground, and strong ionizing radiation and magnetic field are present during collisions. Therefore, the operation of ALICE must be automated as much as possible and the experiment is controled and monitored remotely. The Detector Control System (DCS) controls, verifies, and configures each ALICE's detector equipment. To perform this tasks, the DCS sends commands and reads the status of the equipment from the ALICE Run Control Center (ARC). Alternatively, the DCS can be accessed from outside the ALICE experiment site with any computer connected to internet using the proper credentials for remote operation.

A DCS allows for:

- Correct and safe operation of the ALICE detectors.
- Monitoring the infrastructure and the external systems.
- Integration of sub-detectors in a single central ALICE DCS.
- Configuration of detectors for different data taking strategies (cosmics, p-p, etc.).
- Providing luminosity measurement to the accelerator.

- Providing a chronological record of operating conditions and displaying parameter trends needed for monitoring and physics data reconstruction.
- Automatic recovery of some failures, or exclusion of a faulty channel.

2.2 DCS software

2.2.1 WinCC OA

The DCS for ALICE is based on the WinCC Open Architecture (WinCC OA) software. WinCC OA is a commercial Supervisory Control and Data Acquisition (SCADA) software from ETM Company, which is an owned subsidiary of Siemens AG. SCADA is an industrial control architecture that carries out the supervision task of process control. As such, WinCC OA is a software package designed for the use in automation technology. Its main application is the operation and control of hardware equipment using workstations with full graphical capabilities[13].

The software allows users to visualize current process states and gives the possibility to transfer conditions and commands to the process and its control equipment. The operator uses the mouse, the keyboard and other input devices interactively with an immediately displayed response on the screen. WinCC OA also incorporates and alarm system that displays alerts in case of critical conditions or exceeding of a predefined threshold, a graphical editor to design and customize the graphical user interfaces, and tools to manage data of the process. Particularly important is the archiving of historical data and the possibility to retrieve it and thus use it for later analysis and interpretation.

Datapoints

In order for WinCC OA to monitor a process, the variables involved in that process must be defined and managed by the software. For instance, there has to be a variable that represents the value of every logic state of the process (for example on, off, running, error), every measured value or set value within the system. These variables are called Data Points (DPs) and they're the basic unit of data in WinCC OA.

A data point can store very complex structures of different types of data (string, boolean, float, etc.). Data Points (DPs) are organized in a tree structure that groups together variables from a single device, channel, etc. This structure can have multiple levels and is based on logical connections between the variables. The values of the actual process are saved on data point elements (the outer leaves of this tree structure). Each process variable corresponds to a data point element within a data point. In addition, the tree structure can have as many

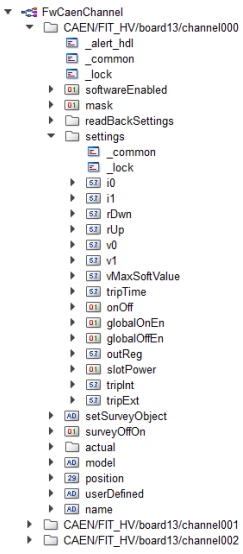

Figure 2.1: Example of a datapoint structure for a high voltage channel

nodes as necessary for a clear organization of the data. Each data point element is addressed individually by the description chain within the structure.

The user may configure and save an appropriate DP tree structure in a Data Point Type (DPT). A data point type serves as a template for the similar data points derived from it. It is always necessary to define an appropriate data point type before creating a data point.

Figure 2.1 depicts a DP for a high voltage channel. In this example, the DPT is FwCaenChannel, a template for a high voltage channel of a CAEN device, and the DP is named CAEN/FIT_HV/board13/channel000, corresponding to a specific high voltage channel of a particular high voltage board. Once this DPT is defined, all the DPs for the rest of the channels will have the exact same structure of the DPT FwCaenChannel, but of course different names (like CAEN/FIT_HV/board13/channel001, visible at the bottom of the figure) and values. This DPT has separate branches for "settings" and "actual", clearly differentiating the values set in the channel and the actual ones delivered by the equipment. These branches are subdivided in electric voltage (v0), electric current (i0), maximum values and ramping steps for those parameters, etc.

GEDI

WinCC OA's Graphical Editor (GEDI) is used for creating and editing panels. It provides tools for creating and configuring graphic objects that can be visual representations of complete systems or just simple operating screens. Furthermore, these graphic objects can be linked with data points.

For example, a change in the status of a process can be shown in an icon representing a device with changing colour surroundings, or in a graphical representation of a switch. It could also be explicitly stated by a message in a text field. On the other hand, changes in process variables can be displayed in trend diagrams, tables, etc.

Managers

The core of a WinCC OA project are the managers. They start all the relevant processes needed for a project to run; for example launching user interface panels, running monitoring scripts in the background, updating datapoints, etc. and they keep said processes separate as autonomous functional units, allowing to spread the work and also making possible to keep certain tasks running while shuting off others. Figure 2.2 depicts the architecture of WinCC OA managers, with the different layers of functions. The managers are:

- Event Manager (EV): There is only one per system. It receives, evaluates and distributes messages (known as events) from and to all other managers.
- Database Manager (DM): Manages the database that reflects your process' status, including archive of the most recently known values/alarms, as well as historical data. It also records the system setup.
- User Interface Manager (UIM): Provides a graphical visualization of messages received by the Event Manager and forwards the user input back to it. It also executes the scripts that contain the code behind the panels.
- Control Manager (CTRL): Executes C++ scripts non-related to panels but rather triggered by events, supported by a large library of functions but also having the possibility of adding new ones.
- Application Programming Interface Manager (API): Allows to incorporate other compiled code in the system.
- Driver Managers (D): They provide a communication protocol between WinCC OA and the hardware devices, performing smoothing and conversion of values, as well as data type transformation (e.g. binary to integer).

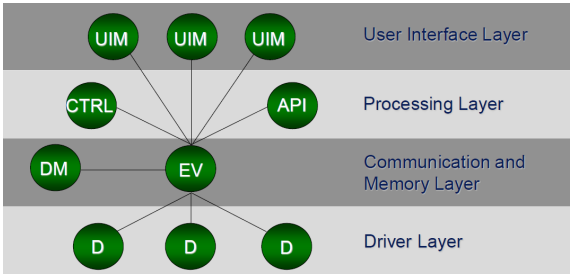

Figure 2.2: Overview of WinCC OA managers architecture

Constant communication between the managers is carried out through the EM. For example, a driver manager receives an update in the state of a hardware device (for instance a change in high voltage values) and sends this information to the EM. The EM, in turn, sends the new values to the DM, which updates the datapoint elements. When these datapoint values are updated, the DM informs the UIM through the EV, and the new values are displayed in the corresponding user interface panel. Inputs in the panel, like pressing an "off" button are sent to the EV and from here, to the DM manager, updating the corresponding DP, and to the hardware devices via the driver managers, turning off the channel.

The EV also might send the incoming information from DM or UIM to the control managers. For example, a control manager script may be designed to monitor magnetic fields, and execute actions, like turning off devices whenever the magnetic field is turned on. DM informs EV of the magnetic field presence, and then it informs the corresponding control manager. Then the control manager gives the indication to driver managers of turning off a device.

Distributed systems

WinCC OA offers a variety of options for developing complex control systems, for instance:

- Single system, Single machine
- Single system, Multiple machines (Scattered system)
- Single Redundant (and split) system
- Many Systems (Distributed system)

In order to keep operation of all systems independent but also be able to share information between them, CERN control systems use the Distributed System

approach, where two or more autonomous WinCC OA systems are connected via network (LAN). Each system can have its own connections to the hardware, and all process data is mapped to local data points only. Data is held only once, anywhere. Systems are capable of displaying (and processing) data from other systems, and this communication can be uni-directional only, if needed. Furthermore, systems can issue commands to hardware connected to another system, and they have direct access to read and write online values, states, alarms or history anywhere in the distributed system. Another kind of manager named the the Distribution Manager provides the interface between systems.

In the ALICE experiment, the distributed system approach allows the subdetectors to access datapoints' information from external systems (LHC, Alerts, Experiment Control System, User Interface) such as environment, beam, safety or gas values, as well as data from other subdetectors.

2.2.2 JCOP Framework

The Joint COntrols Project (JCOP) Framework is a set of tools and components designed to reduce the effort and cost of developing control systems for the four major LHC experiments (ATLAS, CMS, ALICE and LHCb) at CERN.

JCOP provides, supports and maintains a common Framework that facilitate the configuration, monitoring and operation of the different sub-detectors and also include communication mechanisms with the Data Acquisition/Trigger systems, as well as with external systems such as the CERN infrastructure services and the LHC. Experimental equipment such as power supplies and readout devices can easily be integrated in WinCC OA by using JCOP Framework. The Framework is based in and designed specifically for WinCC OA, running as a software package installed within it.

Some of the tools provided by the JCOP Framework are:

- OPC UA Tools. This component assists developers to handle properly connections and subscriptions to commercial devices supporting the OPC UA standard.

- DIM, on the other hand, allows for implementing communication with custom/non commercial hardware devices.

- FSM Tools. This component allows the definition and operation of hierarchies of objects (representing hardware devices or other complex logical entities) behaving as Finite State Machines.

- Device Editor Navigator, allowing easy management, configuration and operation of the devices.

- Trending Tool, allowing the displaying of trending plots for selected parameters.

2.2.3 OPC

OPC (Open Platform Communications), developed by the OPC Foundation, is the standard for the secure and reliable exchange of data in the industrial automation space and in other industries[15]. OPC is platform independent and ensures the seamless flow of information among devices from multiple vendors.

The OPC standard consists in a series of specifications developed by industry vendors, end-users and software developers that define the interface between Clients and Servers, as well as Servers and Servers, including access to real-time data, monitoring of alarms and events, access to historical data and other applications.

The OPC communication requires a device certificated by the OPC foundation and a PC which has an OPC server and OPC clients. OPC clients get data via OPC server. OPC servers are published by manufactures which produce devices users will use.

Among the commercial devices that employ OPC there are the CAEN High Voltage power supply systems which are used in the FIT project. In this case, WinCC OA is the client that communicates with OPC UA CAEN server.

2.2.4 DIM

DIM (Distributed Information Management) is a messaging infrastructure and protocol for information publishing, data transfer and inter-process communications. Like most protocols, is based on the client-server paradigm[16]: Servers provide services to clients, understanding service as a set of data of any type or size. A third element, known as Name Server, keeps an up-to-date directory of all the servers and services available in the system. Figure 2.3 shows how DIM components (Servers, Clients and the Name Server) interact.

Servers publish their services by registering them with the name server. Clients subscribe to services by asking the name server which server provides the service and then contacting the server directly, providing the type of service and the type of update as parameters. Services are normally requested by the client only once (at startup) and they are subsequently automatically updated by the server either at regular time intervals or whenever the conditions change (according to the type of service requested by the client).

The WinCC OA-DIM toolkit allows to interface WinCC OA to hand-made devices (like FIT's newly developed electronics) which do not provide any of WinCC OA's supported protocols (such as OPC).

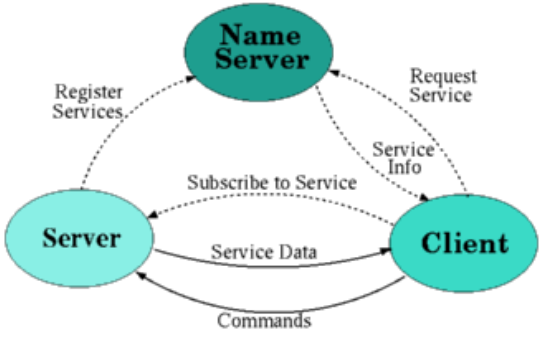

Figure 2.3: DIM architechture

2.2.5 FSM Tools

The FSM toolkit incorporated in the framework is called SMI++ (State Management Interface). The mechanism adopted at CERN for modelling the structure of sub-detectors, sub-systems and hardware components in a consistent fashion is to use a hierarchical (tree like) structure. This tree is composed of two types of objects: Device Units, which are capable of monitoring and controlling the equipment to which they correspond, and Control Units, which can model and control the sub-tree below them. SMI allows the description of any sub-system as a collection of these objects, each one modeled as a Finite State Machine (FSM)[17], meaning that it can be in exactly one of a finite number of states at any given time. The FSM can change from one state to another in response to some inputs, and the change from one state to another is called a transition.

Control Units

Control Units (CUs) are complex, logical decision units comprising DPs (which contain information about label, panel, ownership, exclusivity modes, etc.) and Finite State Machine processes (providing information on objects, states, possible actions, etc.). WinCC OA communicates with the FSM processes via an API Manager - PVSS00smi.CUs can take decisions and act on their children (i.e. send them commands) based on their states. State transitions can be triggered by a command reception (either from its parent or from an operator) or by state changes of its children. Any CU and the associated sub-tree can be a self-contained entity.

State transitions cause the evaluation of logical conditions and possibly commands to be sent to the children. This mechanism can be used to propagate actions down the tree, to automate operations and to recover from error situations.

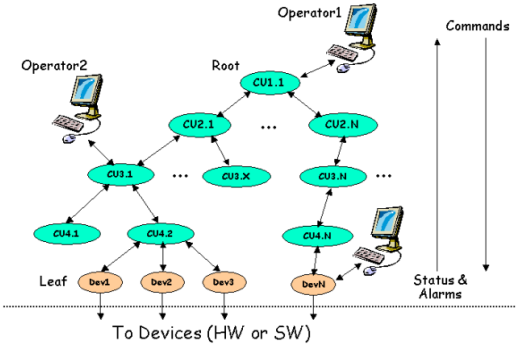

Figure 2.4: Generic controls hierarchy architecture

Device Units

Device Units (DUs) implement the interface with the lower level components of hardware or software of a system. They are always a tree leaf (i.e. they have no children) and they do not implement a complex logic behaviour like CUs, but they still can receive commands and act on the device, or receive device data and translate it into a state. A DU corresponds to a DP of a certain DPT.

Figure 2.4 summarizes the described architecture for a controls hierarchy. In this hierarchy "Commands" flow down and "Status and Alarm Information" flow up.

2.3 DCS hardware

2.3.1 ALF-FRED system

Installation of new FEE for Run 3 required the development of the whole Front-End (FRED) DCS subsystem. The Front-End modules in the ALICE experiment use the CERN developed GigaBit Transceiver (GBT) link to transfer detector signals to the DCS and the O^2 systems. GBT links are controlled by the Common Read-Out Units (CRUs) installed in the First Level Processors (FLP)s.

The Common Read-Out Unit (CRU) acts as the interface between the detectors' electronics, the O^2 facility, the DCS (via the O^2 facility), as well as the trigger, timing and clock distribution systems. CRUs are based on high performance Field Programmable Gate Array (FPGA) processors equipped with multi gigabit optical inputs and outputs. Depending on detector specifications, detector

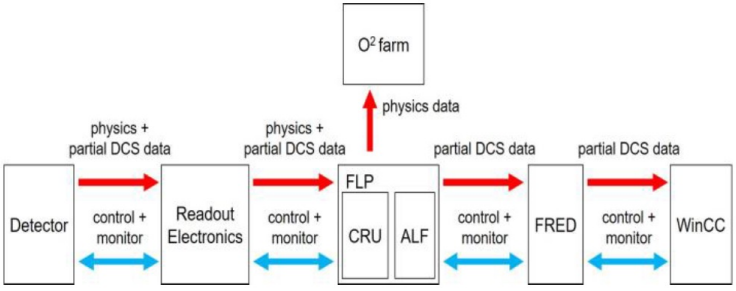

Figure 2.5: The ALF-FRED role in the DCS

data sent to the CRU are multiplexed, processed and formatted. Furthermore, the CRU is capable of multiplexing the data, trigger and control signal over the same GBT1.4.

The ALF-FRED system provides communication between WinCC OA and the detectors' FEE. Figure 2.5 shows the ALF-FRED architecture. The FRED (Front End Device) server applications communicate with detector readout electronics via ALF (ALICE Low Level Frontend) server applications running on FLP computers[18]. FRED provides the translation of high level WinCC OA commands to ALF low level commands and unpacks the ALF data before it is published to the WinCC OA. ALF does not perform any operations with the data and serves only as an interface between the DIM protocol and the detector electronics; it can read/write registers implemented on the front-end modules and publish the data to WinCC using a DIM service. ALF can also receive commands from WinCC and convert them to be sent to the front-end electronics[19].

The FLP servers host several CRU cards, and provide splitting of data transferred over GBT links from the detector electronics into physics and DCS data. The physics data are further sent to the O^2 farm, which tackles the physics processing. DCS data, stripped from the GBT stream, is forwarded to the FRED system.

2.4 ADAPOS

The new DCS for ALICE has been developed to follow the O^2 strategy, with data flow from the DCS to O^2 is managed by the ALICE Data Point Service (ADAPOS). ADAPOS is a software architecture developed for LHC Run 3 whose task is to collect detector's operating conditions data required for the further stages of reconstruction in O^2.

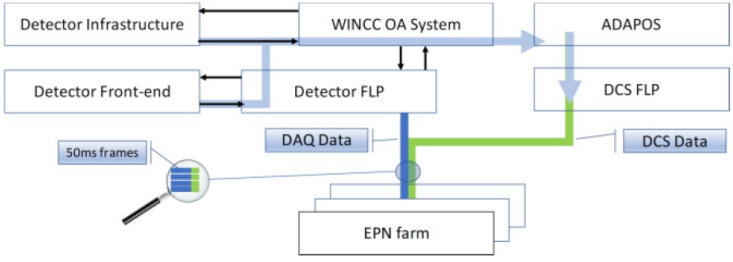

Figure 2.6: The ADAPOS service in the O^2 architecture

When the state of a data point changes in WinCC OA, ADAPOS passes the new value on to the EPN farm of the O^2 facility (Figure 2.6) [20]. This communication is based on the DIM system. For each value, a corresponding DIM service is created, and the published value is updated on each change [19].

Because ADAPOS applications only keep track on the latest known state of each data point, the same memory allocations can be reused. Thus, the memory consumption of ADAPOS applications doesn't increase over time, unless there are recursive memory leaks.

Chapter 3

FDD DCS Hardware Components

This chapter describes the control architecture and the hardware components the FDD DCS controls and monitors, which are:

- The High Voltage (HV) power supply system, consisting of the CAEN crate, the CAEN HV boards and the PMTs. Its purpose is to amplify and transform the light produced by FDD into electrical signals.
- the Front-End Electronics (FEE) system consisting of the Wiener crate, the Trigger and Clock Module (TCM) board and the Processing Module (PM) boards. Its main purpose is to process and analyze the signals coming from the HV system and produce the trigger signals for the other ALICE detectors.
- The Laser Calibration System (LCS), consisting of a dedicated PMT, an optical attenuator and a laser source. Its purpose is to carry out calibration measurements and monitor the performance of FDD over time.

3.1 Control architecture

FDD-DCS adopted a control architecture[21] for its hardware based on the one used by the ALICE experiment, composed of the supervision, control, and field layers. The supervision layer consists of Operator Nodes (ON) in the ALICE Control Room, that provide the operator interface to interact with the control layer, where the Worker Nodes (WN) interface to the experimental equipment[1].

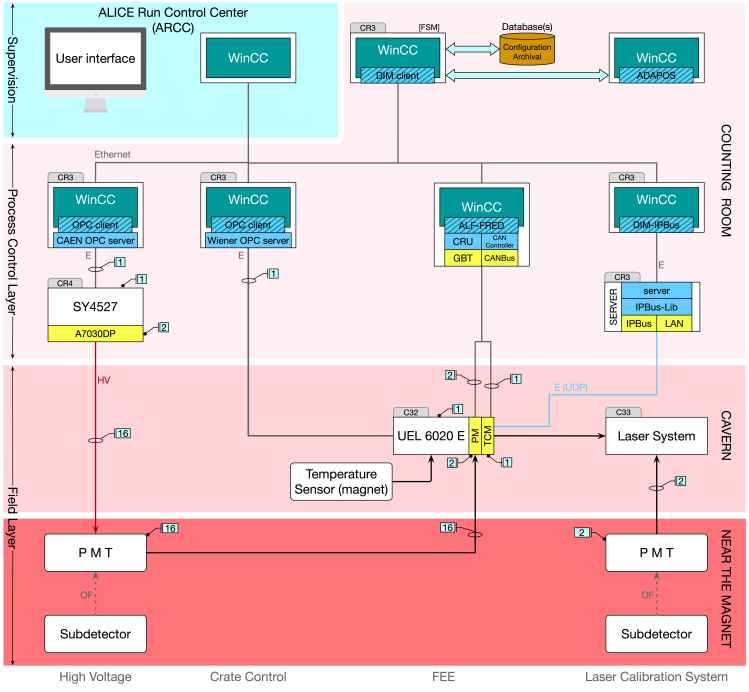

Figure 3.1: FDD control architecture

It is in the WNs where the actual WinCC projects for each detector are installed and developed by experts. The WNs collect, and process information from the lower layer called the field layer and make it available for the supervisory layer for monitoring purposes. The WNs also receive information from the supervisory layer to be processed and distributed to the field layer, for example on/off commands. The field layer consists of the hardware devices to be controlled; it can include power supplies, crates, sensors, actuators, and, in general, any device acquiring physics, environmental, conditions, configuration or other kind of data. The FDD control architecture is illustrated in Figure 3.1.

3.2 High Voltage

The High Voltage system powers the photomultiplier tubes that are connected to the FDD plastic scintillator modules. For this, FDD uses the Universal Multi-channel Power Supply CAEN crate SY4527 (Figure 3.2), which can accommodate

Figure 3.2: Universal Multichannel Power Supply CAEN crate SY4527.

Figure 3.3: High voltage board CAEN A7030DP.

up to sixteen high voltage boards in it. The model of the boards installed in the crate is CAEN A7030DP[22] (Figure 3.3). These boards provide up to 12 high voltage channels, and the output voltage can be set from 0 to 3 kV with a maximum power of 1.5 W per channel[23]. FDD uses two of these boards, one for each station.

3.2.1 PMTs

The core of the HV system is the set of PMTs. A PMT is a tube-shaped device with a photocathode in one of its end that detects tiny light signals and produce electrons via photoelectric effect. A high voltage source applies an electric field in the tube, accelerating the electrons. Using dynodes, the signal is further amplified via several succesive electron re-emissions.

In FDD, the PMTs collect the light signals produced by the plastic scintillator modules and send the resulting electrical signals to the FEE. There are 19 PMTs in total: one for each module, one reference PMT per station, and one PMT for the LCS. Therefore, 19 high voltage channels from A7030DP boards are required to power the PMTs; nine high voltage channels from each board are used per FDD station, and the LCS PMT uses an extra channel from FDD C board.

All of FDD PMTs correspond to the H8409-70 model by Hamamatsu (Figure 3.4), designed specifically for use in environments with high magnetic fields of the order of Teslas, which makes it ideal for its use in the ALICE experiment. This PMT has a fine mesh dynode structure (with 19 dynode stages), a round

Figure 3.4: Hamamatsu H8409-70 photomultiplier tube.

photocatode made of bialkali with a diameter of 27 mm, and a gain of $1{\times}10^7$. The absorbance spectrum ranges from 300 nm to 650 nm with a peak at 420 nm[24].

3.3 Laser Calibration System

The LCS scheme for FDD is shown in Figure 3.5. The signal from the laser source is regulated via an optical attenuator, and is then forwarded to the main reference PMT. This reference PMT is directly radiated using a partially open patch cord. An optical switch allows for channeling the signal into one of two directions: the PMTs or the plastic scintillator modules, and optical splitters divide the signal to reach each one of the modules/PMTs, as well as the reference PMTs which are located one in each FDD station. The LCS was successfully used in the commissioning of FDD. Additionally, it will contribute to monitor ageing of the detector and perform calibration measurements prior to each run, which is necessary to ensure accurate data collection.

3.4 Front-End Electronics

The Front-End Electronics (FEE) system of FDD processes the signals from the PMTs and generates trigger signals for ALICE. The INR members of the FIT collaboration developed the FEE that all three subdetectors use [25][26]. The FEE consists of two types of boards: Trigger and Clock Module (TCM) and Processing Module (PM). One PM can receive and process up to 12 independent signals directly from detectors' photosensors, and a single TCM can handle data from up to 20 PM modules. Therefore, each detector uses one TCM and as many PMs as needed depending on the number of detector channels. For FDD, two PM boards (one for each station) are used.

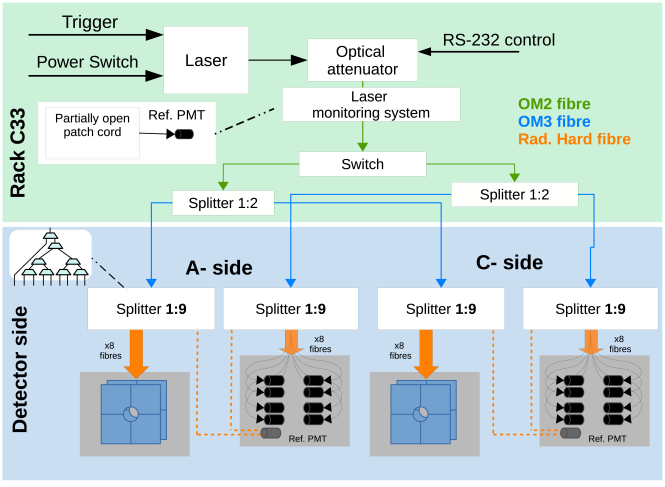

Figure 3.5: Laser calibration system for FDD.

Each PM is connected to the TCM via an HDMI cable to transmit pre-trigger data, slow control data, and the LHC clock signal (which is necessary to synchronize the FEE with LHC particle bunches). The primary task of the TCM is to generate the online trigger signals.

Analog signals from PMTs are input to the PM board. The arrival time and the integrated charge of the pulse are digitized by the Time to Digital Converters (TDC) and the Analogue to Digital Converters (ADC). The digitized data is sent to the CRU for storage and additional processing by the ALICE O2 system. Both PM modules send the pre-trigger data to the TCM, consisting of the sum of amplitudes, times, and the number of active channels in the event. The TCM compares the total from both (but separately) FDD-A and FDD-C arrays with the two predefined threshold values and generates the Central and Semi-Central trigger signals. If at least one event is registered on any side of the FDD subdetector, the TCM generates Or A/Or C triggers. The TCM also generates a Vertex trigger (TVX) signal if the average time difference between FDD-A and FDD-C events is within the predefined time interval thresholds, indicating the longitudinal position of the IP is within the required range interval. The trigger signals are sent to the ALICE Central Trigger Processor (CTP). The TCM also delivers commands and configuration through the 1 Gb ethernet optical link via IP-BUS protocol and transmits essential parameters to the DCS, such as event counters.

The FEE modules are inserted in a dedicated VME crate which is also connected to the CERN network via Ethernet.

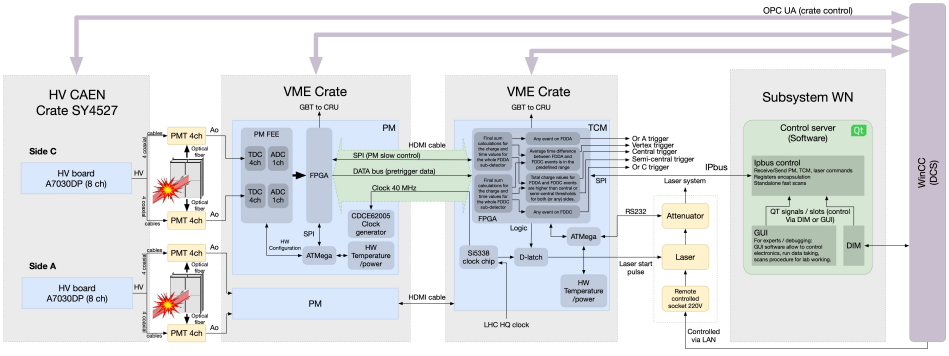

Figure 3.6: Front-End Electronics scheme for FDD.

3.4.1 Control Server

The Control Server is a software application designed to configure, control and monitor the FIT FEE boards. The Control Server was developed by the FIT collaboration using the Qt framework. This software uses UDP-based IPbus protocol to communicate with electronics firmware using a local area network. IPbus is a control protocol for FPGA based hardware devices, which is the case of the PM and TCM boards. The Control Server provides a user interface (Figure 3.7) that allows to manually set configuration parameters and monitor real time values in the TCM and PM boards, for instance:

- Set time windows and electric charge thresholds for the incoming signals in the PMs
- Activate/deactivate and configure trigger generation in the TCM
- Set values for the laser attenuator and laser frequency.
- Display real time rate counts for time and charge of the incoming signals, useful to manually adjust and set proper configuration parameters during calibration of the FEE.
- Display the status of the boards, such as “ready” or “error”, as well as their temperature.
- Buttons to reset and restart the system.

The Control Server also features the saving and loading of configuration recipes to/from file [25]. This way, several FEE configuration settings for different scenar-

ios can be saved and be quickly loaded whenever necessary. The size of the recipe files is 5 Kb and the approximate number of parameters to configure is 455.

3.5 DCS-hardware integration

Integration between the DCS software (i.e. the FDD WinCC project) and the hardware devices is necessary to be able to operate and monitor those devices from the DCS. The OPC UA CAEN server links WinCC OA and the CAEN devices (crate and boards). This server, installed in the FDD DCS WN, communicates with the OPC UA client running in the WinCC project, which is also installed in the FDD DCS WN. The CAEN crate and the FDD DCS WN are both connected to the ALICE DCS network, allowing communication between the OPC UA CAEN server and the crate. Finally, the crate provides control and configuration for the HV boards. Using an analogous procedure, the FEE Wiener crate communicates with WinCC OA through the OPC UA Wiener server.

The FEE boards and laser system, on the other hand, are indirectly linked to WinCC via the DIM protocol and the Control Server. The TCM board controls the PMs, laser source and attenuator. As seen in Figure 3.6, the Control Server (installed in the FDD DCS WN) communicates with the TCM board via IPbus protocol and with the WinCC project via DIM services and commands.

As stated in section2.2.1, WinCC manages all the data in the variables of a monitored process through datapoints, meaning that the WinCC OA and JCOP Framework tools to develop panels, Finite State Machines, alarms, etc. work only with datapoints and not with the hardware devices directly. This means that, for each variable or parameter related to the FDD DCS hardware components, a corresponding datapoint element within the appropriate datapoint type must exists in the FDD WinCC project. After completion of the DCS-hardware integration process, these datapoints update in real time according to the hardware status, and they provide the link between the devices and the control panels, Finite State Machines, ADAPOS, alarms, archiving, etc.

All the required datapoint types and datapoints that model the FDD hardware variables were created and configured in the FDD WinCC project. These datapoints include for example:

- Physical and logical status of the crates, boards, attenuator, laser source and PMTs: wether they're on/off, ready/not ready, OK/in error, their temperature level, etc.

- Settings and actual values for the HV and PM boards parameters, like high voltage, current level, time window, charge threshold, etc.

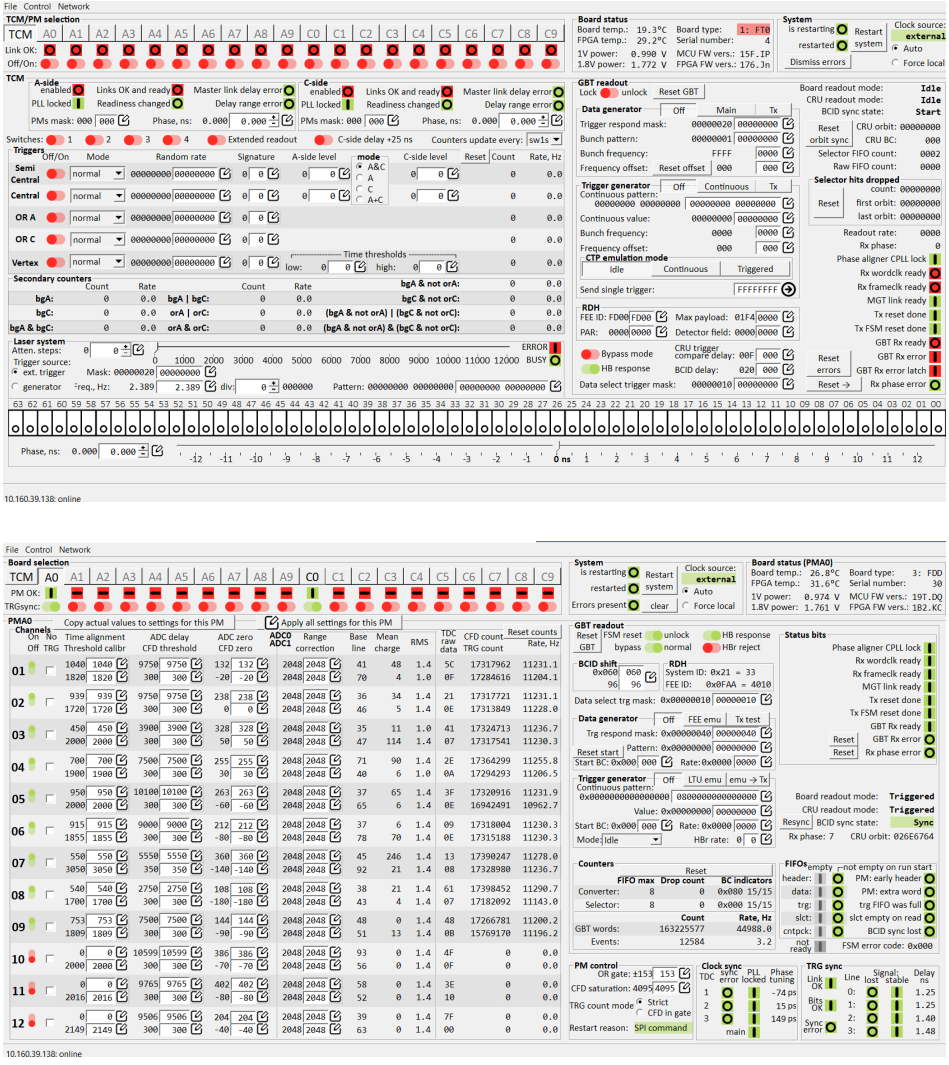

Figure 3.7: Control Server user interface. Top: TCM tab and controls. Bottom: PMA0 tab and controls

- Controls to execute actions in the FEE such as restart, shut down or clear errors.
- Values of the triggers generated by the FEE.
- Rate count event of the PM channels.

Integration of the HV system to the DCS was tested before installation using the actual CAEN devices to be installed in the ALICE experiment and a personal computer running WinCC OA and the OPC server. Tests were successful, and the CAEN devices were later installed and integrated to the FDD DCS project. On the other hand, after the INR team configured the DIM services and commands for the FEE, said services and commands were linked to their corresponding datapoints in the WinCC project.

Chapter 4

Control model and User Interface for FDD DCS

4.1 Software architecture

Figure 4.1 shows the logical control hierarchy for FDD DCS [21]. Such hierarchy was designed based on the FIT project standards and the hardware architecture of FDD, i.e., based on the physical components of the detector. Therefore, the control hierarchy has two sub-trees for the A and C side detector arrays monitoring their corresponding PMTs and PMs, and additional sub-trees for the rest of infrastructure items: the TCM board, the Laser Calibration System and the HV and FEE crates. The Control Server software has also its own sub-tree. Elliptical nodes indicate Control Units and rectangular nodes indicate Device Units. Each node in the hierarchy was modeled and configured as a Finite State Machine (FSM). Therefore, each node has a finite number of states to be in and a set of

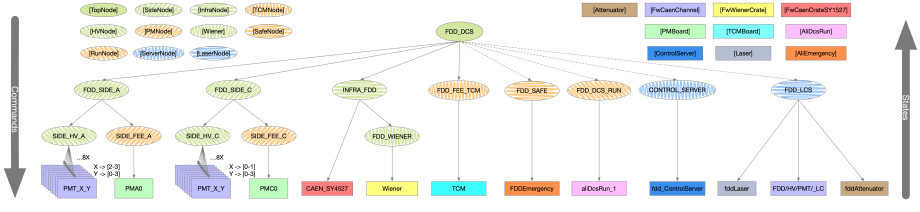

Figure 4.1: FDD DCS software architecture

commands that can be executed. The state a node is in depends of a series of conditions, which in this case are the states of the children. Whenever a node executes a command, further commands are sent to its children, who might change their states. On the other hand, whenever a child changes its state, it reports this change to its parent, who might in turn transition to another state. FDD_DCS is the top node in the hierarchy. Commands are sent in parallel from this node to all lower sub-trees, and they report their states to the top node to reflect the overall state of the FDD subdetector.

To develop the complex control system, the control hierarchy, and its states, as well as their transitions and conditions for them were defined first. Then the commands that execute actions on each node were defined. The ALICE controls coordination is in charge of the central ALICE DCS execution, and as such, it defines the guidelines and standards for the subdetectors' FSMs. The top FSM node of all subdetectors must use common states, so that the central ALICE DCS has only to interact with a common FSM type with the same states and actions for all the subdetectors. This also allows any non-expert operator of the Central DCS to control the subdetectors[27]. On the other hand, the states of all other nodes can be determined freely by each subdetector according to their specific hardware and software required conditions for operation (the SAFE and RUN sub-nodes are exceptions; according to ALICE guidelines, these branches must be implemented under the top node and also be identical in their states and actions for all subdetectors).

The design of the control hierarchy goes from the top-level node (CU) to the lowest level (DU), i.e., top-down approach, to come up with the overall tree-like structure. On the contrary, the design of the DU FSMs states and their transitions were designed first, taking into account the configuration parameters and the data the modeled devices produce. Then, the CU FSMs and the top node were designed, maintaining consistency with the corresponding higher level FSMs, i.e., bottom-up approach. Therefore, a combination of top-down and bottom-up strategies was used during the development phase.

4.2 Top level node

The top node in the hierarchy is the control unit FDD_DCS. Its children nodes are FDD_SIDE_A, FDD_SIDE_C, INFRA_FDD, FDD_FEE_TCM, FDD_SAFE, FDD_DCS_RUN, CONTROL_SERVER and FDD_LCS (Figure 4.2). FDD_SIDE_A and FDD_SIDE_C control the PMTs power and supervise the PM boards. INFRA_FDD controls both the high voltage boards and the crates that accommodate the high voltage, PMs, and TCM boards. FDD_FEE_TCM monitors the state of the TCM board, and FDD_LCS does the same for the laser calibration system

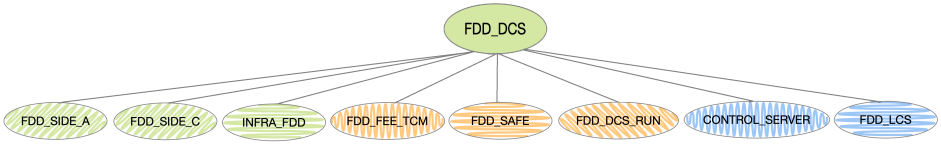

Figure 4.2: Sub-tree below FDD top node

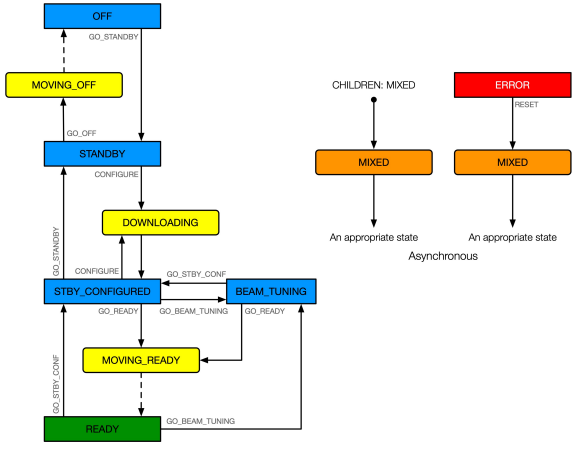

Figure 4.3: State diagram for FDD_DCS node

(attenuator, laser and reference PMT). Lastly, FDD_SAFE and FDD_DCS_RUN control the Device Units responsible of monitoring FDD's Safety condition and readiness for data taking, respectively.

Figure 4.3 shows the state diagram of the top node. It describes the possible states of the node and the possible commands to execute actions and/or trigger state transitions. The states are divided into synchronous states used in regular operation and asynchronous states reflecting anomalous situations. The top node states follow the ALICE standard states[27]. The devices status corresponding to each synchronous state in FDD_DCS is as follows:

i) OFF. The HV power supply channels are powered off, and the FEE are not ready.

ii) STANDBY. The HV power supply channels remain powered off, but the FEE are powered on.

iii) DOWNLOADING. All configuration data is being downloaded from the database to the devices.

iv) STBY_CONFIGURED. The devices are configured. The condition of the

equipment and systems is the same as in STANDBY.

v) BEAM_TUNING. A safe detector mode whenever the beam is being injected into the LHC. The HV power supply channels are powered on but are not yet ready to supply power to the PMTs of the FDD subdetector.

vi) MOVING_READY. The voltage levels of the HV power supply channels are ramping up.

vii) READY. The PMTs and FEE are powered and configured, and the FDD can start taking data.

viii) MOVING_OFF. The voltage levels of the HV power supply channels are ramping down and the FEE are being powered off.

The meaning of the asynchronous states used in FDD is as follows:

i) MIXED. If the child nodes of any node do not have all the same state, the parent node goes to the MIXED state. For example, one case would be if some power supply channels are in the "ON" state and others are in the "OFF" state. ii) ERROR. If a child node of any node is in ERROR state, the parent goes to ERROR state. For example, if the child is a DU connected to a device that is in some malfunctioning situation, the parent goes to ERROR.

The association between the parent's state transition and those of the children is described in the synchronization Table 4.1. This table shows what are the conditions (i.e. the states) that the children nodes have to met for their parent to be in a certain state. The FDD_DCS states are listed in the STATE column. The corresponding states of the children are shown in the columns under CONDITIONS. For example, the first state of FDD_DCS is OFF, since FDD_SIDE_A, FDD_SIDE_C, INFRA_FDD, and FDD_FEE_TCM are all in state NOT_READY. When FDD_DCS is in state OFF, the GO_STANDBY command can be executed, as seen in the state diagram; consequently, FDD_SIDE_A and FDD_SIDE_C go from NOT_READY to STANDBY, meanwhile INFRA_FDD, and FDD_FEE_TCM go from NOT_READY to READY. FDD_SIDE_A/C eventually go to READY too by executing subsequent commands according to the state diagram in regular operation. Therefore, also the state of FDD_DCS goes down from OFF to READY as shown in Table 4.1. The upper rows above the empty row (OFF to READY) refer to synchronous states, and the lower rows (e.g., MIXED and below) refer to asynchronous states. An empty cell means any different synchronous state. For example, when FDD_SIDE_A is in ERROR, FDD_DCS goes to ERROR, regardless of the state the rest of the nodes are in. FDD_SAFE and FDD_RUN are not included in this table since they're not hardware-related nodes but rather special nodes required by ALICE whose state doesn't affect their parent directly.

The HV, PM and TCM configuration is done during DOWNLOADING state of the FSM by loading predefined recipes in Control Server and the CAEN high voltage boards.

STATE	CONDITIONS					
FDD_DCS	*FDD_SIDE_A*	*FDD_SIDE_C*	*INFRA_FDD*	*FDD_FEE_TCM*	*CONTROL_SERVER*	*FDD_LCS*
OFF	NOT_READY	NOT_READY	NOT_READY	NOT_READY	NOT_READY	OFF
MOVING_OFF	MOVING_OFF	MOVING_OFF	READY	READY	NOT_READY	NOT_READY
STANDBY	STANDBY	STANDBY	READY	READY	READY	STANDBY
DOWNLOADING	STANDBY	STANDBY	READY	READY	READY	STANDBY
STBY_CONFIGURED	STBY_CONFIGURED	STBY_CONFIGURED	READY	READY	READY	STANDBY
BEAM_TUNING	BEAM_TUNING	BEAM_TUNING	READY	READY	READY	STANDBY
MOVING_READY	MOVING_READY	MOVING_READY	READY	READY	READY	READY
READY	READY	READY	READY	READY	READY	READY
MIXED		MIXED				
ERROR		ERROR				

Table 4.1: Synchronization table for FDD_DCS.

4.2.1 Top level node user interface

This text describes the main user interface of the FDD FSM top node, including its structure, color-coding conventions, and available commands.

Figure 4.4 is the main user interface of the FDD FSM top node. The top left corner of the panel is a JCOP Framework standard section present in all the FSM panels that reflects the FSM structure and state. It shows a two column list with the name and state of the current node and all of its children sub-nodes. The states are coloured according to ALICE's convention for operation in order to be understandable by the central DCS operator. Table 4.2 describes the meaning of these colours.

STATE	DESCRIPTION	COLOUR	FRAMEWORK COLOUR
READY	OK and in physics data taking	Green	FwStateOkPhysics
BEAM_TUNING, STBY_CONFIGURED, STANDBY, OFF	OK but not in physics data taking	Blue	FwStateOkNotPhysics
DOWNLOADING, MOVING_READY, MOVING_OFF	In a transition state, temporary low level severity, will resolve itself	Yellow	FwStateAttention1
MIXED	Inconsistent state, unable to take data, must be cured by DCS operator or detector expert	Orange	FwStateAttention2
ERROR	Error state, must be cured by DCS operator or detector expert	Red	FwStateAttention3

Table 4.2: Colour convention for ALICE detectors top node states

Every node has also a lock icon that indicates availabilty to control it. A lock can be "free", in which case it will appear open, or "taken", in which case it will appear closed and coloured red. For the user holding the lock the colour will be green. Clicking on the states' labels opens a drop-down list with the available commands for that specific node, and if the operator is the holder of the lock,

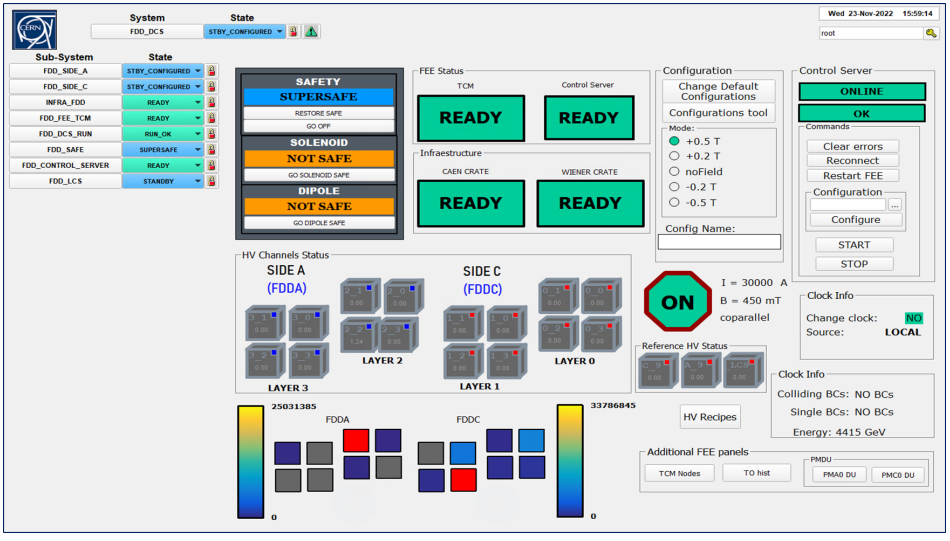

Figure 4.4: FDD DCS main user interface

such commands can be executed.

The rest of the elements distributed in a rectangular fashion make up the actual custom panel. The top left section displays the safety state of the FDD (SAFE, SUPERSAFE, or NOT SAFE) with respect to the LHC beam status, according to the state of the node FDD_SAFE. The safety state of the FDD regarding the ramping state of the ALICE magnets (dipole and solenoid) is also shown. Finally, buttons linked to the Safety scripts allow the user to execute the actions defined in those scripts: RESTORE SAFE, GO SAFE, GO SUPERSAFE, GO DIPOLE/SOLENOID SAFE and RESTORE FROM DIPOLE/SOLENOID SAFE.

The “FEE Status” and “Infrastructure” sections at the top center display the readiness of the TCM board, Control Server software, HV crate and FEE crate, making easy to detect at a glance which of the essential elements for operation are or not ready.

The “HV Channels Status” section at the middle is a graphical representation of both sides of the FDD subdetector, showing the position of each layer and scintillator module with respect to each other. Each module is labeled with its corresponding PMT number and displays the monitored voltage level, giving a quick general visual of the subdetector state.

Overall, this main panel allows the user to easily visualize, monitor, and change the state of the main elements of the system.

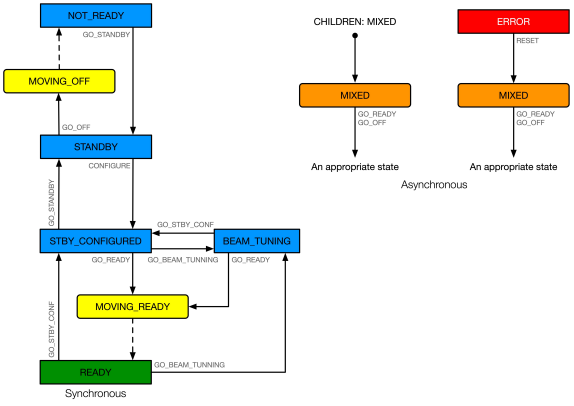

Figure 4.5: State diagram for FDD_SIDE_A and C node.

4.3 Overview of FDD SIDE node and sub tree

The sub-tree under FDD_SIDE_A, shown in Figure 4.6, has two Control Units, _SIDE_HV_A and _SIDE_FEE_A, as children. They show the states of the PMTs HV and of the PM board reading out the scintillator modules on side A (FDD-A). Figure 4.5 shows the state diagram of FDD_SIDE_A, and Table 4.3 the synchronization table. The states of FDD_SIDE_A are listed in the STATE column. The states of the _SIDE_HV_A and _SIDE_FEE_A children are shown in the columns under CONDITIONS. The first state of FDD_SIDE_A is NOT_READY corresponding to the same state of both of its children. Executing the GO_STANDBY command from FDD_SIDE_A in NOT_READY state makes _SIDE_HV_A to propagate this command to its children. During normal operation FDD_SIDE_A is brought to the READY state by sending subsequent commands (CONFIGURE and GO_READY, for example) which makes _SIDE_HV_A and _SIDE_FEE_A end up in the READY state as well. The upper rows in Table 4.3 above the empty row (from NOT_READY to READY) refer to synchronous states, and the lower rows (e.g., MIXED and ERROR) refer to asynchronous states. An empty cell means any different synchronous state. For example, when _SIDE_HV_A is in ERROR, FDD_SIDE_A goes to ERROR, regardless of the state _SIDE_FEE_A is in.

4.3.1 Graphical user interface for FDD SIDE

The graphical user interface for FDD_SIDE_A is shown in Figure 4.7. Esentially, it is a more detailed version of the HV Channel Status section of the main user interface that displays the voltage and electric current levels for each PMT. This

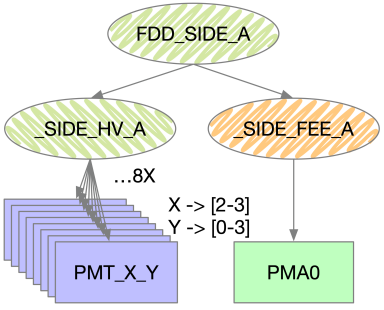

Figure 4.6: Sub-tree below FDD_SIDE_A node

STATE	CONDITIONS	
FDD_SIDE_A (C)	*SIDE_HV_A (C)*	*SIDE_FEE_A (C)*
NOT_READY	NOT_READY	NOT_READY
MOVING_OFF	MOVING_OFF	NOT_READY
STANDBY	NOT_READY	READY
STBY_CONFIGURED	NOT_READY	READY
BEAM_TUNING	STANDBY	READY
MOVING_READY	MOVING_READY	READY
READY	READY	READY
MIXED	MIXED	
ERROR	ERROR	

Table 4.3: Synchronization table for FDD_SIDE_A and FDD_SIDE_C.

control panel allows the user to directly modify the set values of these parameters, either individually or globally, without the need of accessing lower FSM nodes. The control panel for FDD_SIDE_C is identical to this panel. These graphical interfaces also include buttons pointing to another user interface for the reference PMTs (labeled as “spares”) and buttons to display trending plots for voltage and current levels.

4.3.2 High voltage node

The node _SIDE_HV_A supervises the high voltage power supply coming from the A7030DP board in slot 14 of CAEN crate. It has eight PMT_X_Y DUs that interact with the FSMs of channel 000 to channel 007 of the HV board. Figures 4.8 and 4.9 are the state diagrams for _SIDE_HV_A and PMT_X_Y, respectively. Table 4.4 shows the synchronization between PMT XY DUs and their parent control unit. For side C, X goes from 0 to 1, and for side A, X goes from 2 to 3. Y goes from 0 to 3. As seen, all PMTs must be in the same state for their parent node to be in a synchronous state. For example, when _SIDE_HV_A is in

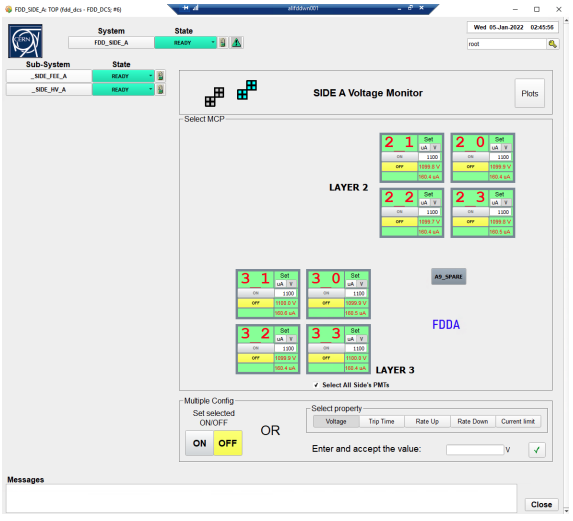

Figure 4.7: FDD side A user interface

NOT_READY state, all PMTs must be in OFF state. Whenever any PMT is in a different state from the rest, the parent goes to MIXED state, and whenever any PMT is in ERROR, TRIPPED or WARNING states, the parent goes to ERROR state, regardless of the state of the rest of the children.

STATE	CONDITIONS	
SIDE_HV_A/C	*PMT_X_Y*	*PMT_X_Y*
NOT_READY	OFF	OFF
MOVING_OFF	RAMPING_DOWN	RAMPING_DOWN
STANDBY	INTERMEDIATE	INTERMEDIATE
MOVING_READY	RAMPING_UP	RAMPING_UP
READY	ON	ON
MIXED	OFF	
MIXED	RAMPING_UP	
MIXED	RAMPING_DOWN	
MIXED	INTERMEDIATE	
MIXED	ON	
ERROR	TRIPPED	
ERROR	WARNING	
ERROR	ERROR	

Table 4.4: Synchronization table for _SIDE_HV_A and C.

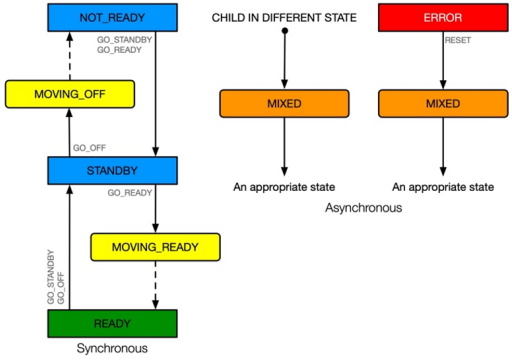

Figure 4.8: State diagram for _SIDE_HV_A and C nodes.

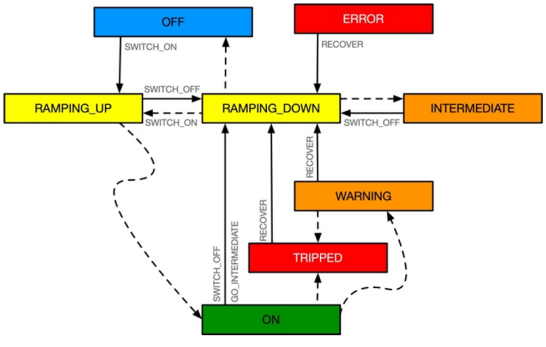

Figure 4.9: State diagram for PMT_X_Y DU.

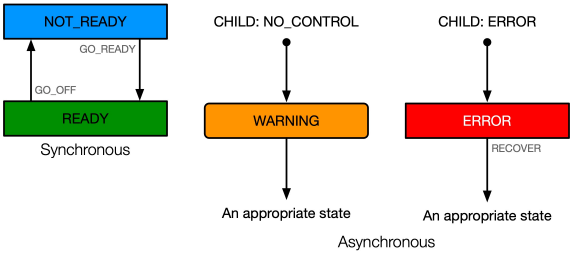

Figure 4.10: State diagram for INFRA_FDD node.

4.4 Overview of Infrastructure node and sub tree

The sub-tree under INFRA FDD in the monitoring system is shown in in Figure 4.11. This node has a Device Unit CAEN_SY4527 and a Control Unit FDD_WIENER as children, reflecting the current states of the crates where the high voltage (A7030DP) and electronics (PMs and TCM) boards are installed, respectively. Figure 4.10 shows the state diagram for INFRA_FDD, and Table 4.5 the synchronization table. The INFRA_FDD states are listed in the STATE column, and the states of CAEN_SY4527 and FDD_WIENER in the columns under CONDITIONS. The NOT_READY state of INFRA_FDD occurs whenever CAEN_SY4527 and FDD_WIENER are OFF and NOT_READY, respectively. In this state the GO_READY command can be issued (see Figure 4.10), making the FDD_WIENER state to change from NOT_READY to READY and the CAEN_SY4527 state to change from OFF to READY. Consequently, the INFRA_FDD state changes from NOT_READY to READY too. The first three rows of the synchronization table correspond to synchronous states, while the remaining rows indicate asynchronous states such as WARNING and ERROR. As before, an empty cell means any synchronous state. For example, when FDD_WIENER is in the state NO_CONTROL, INFRA_FDD should go to WARNING regardless of the state CAEN_SY4527 is in.

STATE	CONDITIONS	
INFRA_FDD	*CAEN_SY4527*	*FDD_WIENER*
NOT_READY	OFF	NOT_READY
NOT_READY	OFF	READY
READY	READY	READY
WARNING	NO_CONTROL	
WARNING		NO_CONTROL
ERROR	ERROR	
ERROR		ERROR

Table 4.5: Synchronization table for INFRA_FDD.

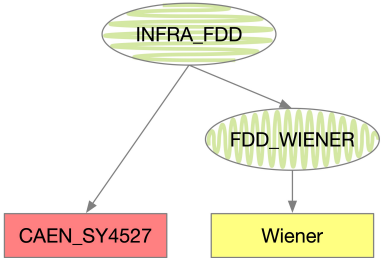

Figure 4.11: Sub-tree below INFRA_FDD node.

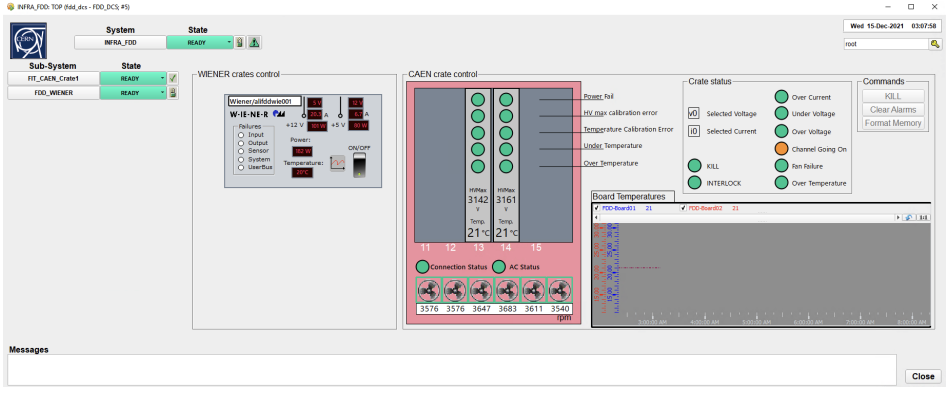

Figure 4.12: Infrastructure user interface

4.4.1 Graphical user interface for Infrastructure node

The infrastructure control panel displays a graphical representation of the Wiener and CAEN crates, as shown in Figure 4.12. Since the crates are installed in the ALICE cavern and its main physical controls and monitoring indicators cannot be accesed or seen, this panel intends to fulfill that purpose for the operator. Several parameters are displayed, such as board temperature and fan speed for CAEN crate, voltage, temperature and current for Wiener crate. Both crates have "LEDs" indicating critical failures that can help to identify error sources and take proper actions. There is also a switch to turn the Wiener crate on/off. As an additional feature, the panel displays trending plots for the temperatures of the HV CAEN boards.

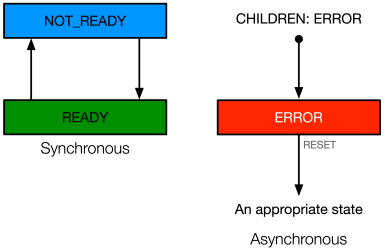

Figure 4.13: State diagram for FDD_FEE_TCM node.

4.5 Trigger and clock module node

FDD_FEE_TCM node has one DU named TCM as its only child. This DU models the Trigger and Clock Module board (TCM) installed in the Wiener crate. The TCM controls the LCS, monitors the PM boards, and generates the trigger signals, hence the importance of having a dedicated node right under the top node.

Figure 4.13 shows the state diagram for FDD_FEE_TCM. The states for the TCM DU (OFF, READY and ERROR) directly correspond to the states of its CU parent FDD_FEE_TCM (NOT_READY, READY and ERROR, respectively); thus, their state diagram is essentially the same. Whenever the Wiener crate is turned on, it powers the TCM board and the state of the TCM DU node changes from OFF to READY. As a result, the FDD_FEE_TCM changes its state from NOT_READY to READY. NOT_READY and READY are synchronous states and ERROR is an asynchronous state. Unlike the other nodes previously described in this chapter, these nodes have no custom user interface panels and their panels just display the JCOP Framework standard section present in the top left corner of all other panels.

4.6 Laser Calibration System node

The sub-tree under FDD_LCS in the monitoring system is shown in Figure 4.14. It has three DUs as children (fddLaser, fddAttenuator and FDD/SIDE_C/HV_C32), that model the states of the LCS system elements that are located in the FIT electronics rack C32 of the ALICE cavern (laser source, optical attenuator, and the main reference PMT).

Figure 4.15 shows the user interface of the LCS node. It allows to monitor and modify voltage and current and access their respective trending plots for the three reference PMTs. This panel also borrows some elements from the Control Server graphical user interface: the state of the attenuator and laser are visible

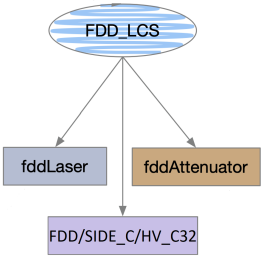

Figure 4.14: Sub-tree below FDD_LCS

and the attenuation steps can be modified. Laser can be turned on/off. Frequency and delay for the laser are also visible. Finally, the panel includes the main PMs readings (time alignment, threshold calibration, ADC delay, and ADC zero, CFD threshold) for the channels corresponding to the three reference PMTs.

4.7 Control Server node

The CONTROL_SERVER node has one DU fdd_ControlServer as child that monitors the state of the Control Server software. The Control Server is the only means to control and configure the PM and TCM boards. Even if the Wiener crate and the boards are on and in READY state, they cannot be properly configured and be ready for data taking unless the Control Server is open and running, hence the need for this node. Figure 4.16 shows the state diagram for this node. The state diagram for its DU child has the same exact structure and it just changes the names of the states and actions. There are only two possible synchronous states, READY when the Control Server is running and NOT_READY in case is not. Executing the command START launches the Control Server and opens its graphical user interface. If the FEE is on, the Control Server immediately communicates with the boards and displays their state and parameters. Command STOP kills the Control Server and closes the graphical user interface.

4.8 SAFE and RUN nodes

The SAFE node is a part of the ALICE Safety Matrix and indicates the safety condition of the FDD detector. Unlike the other nodes, it is not dependent on its children but rather on a combination of conditions from all FDD sub-systems. Conversely, a change in the state of this node affects the rest of the subsystems, even if they are not directly related in the hierarchy.

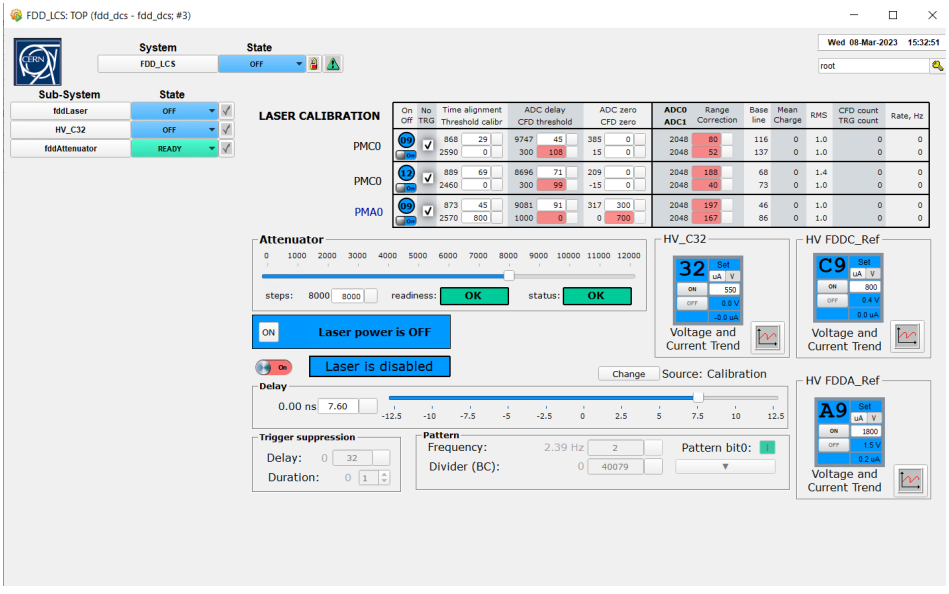

Figure 4.15: LCS user interface

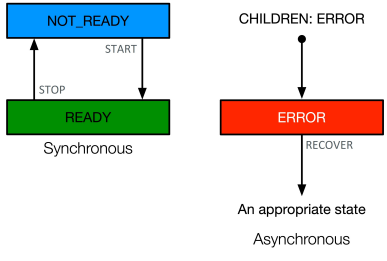

Figure 4.16: State diagram for CONTROL_SERVER node.

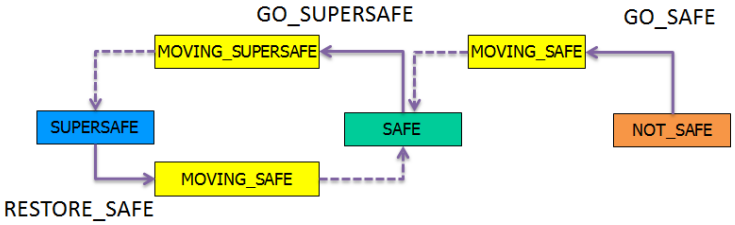

Figure 4.17: State diagram for FDD_SAFE node.

Figure 4.17 shows the state diagram for FDD_SAFE node. The meaning of the colours is somewhat different from the rest of the nodes; for example orange, corresponding to NOT_SAFE, is actually the state for which FDD_DCS is usually in READY (green), and SAFE, which is green, corresponds to FDD_DCS being in BEAM_TUNING (blue). This is further visible in Table 4.6, which depicts the Safety condition of FDD (and therefore the SAFE node state) with respect to its subsystems.

FDD SAFE CONDITION	HV CAEN CRATE	HV CHANNELS	VME CRATE	TOP NODE STATE
NOT_SAFE	ON	ON (V >0)	ON	READY
SAFE	ON	ON (V = 0)	ON	BEAM_TUNING
SUPERSAFE	ON	OFF	ON	STBY_CONFIGURED
	ON	OFF	OFF	OFF
	ON	OFF	ON	STANDBY
MAGNET SAFE	ON	OFF	OFF	OFF
NOT MAGNET SAFE	ON	ON (V = 0)	ON	BEAM_TUNING

Table 4.6: FDD_SAFE node states table.

The RUN node of the FDD detector changes its states as a reaction to the ALICE ECS (Experiment Control System) issued commands. The ECS is the ALICE system in charge of configuring, starting and ending runs. When a run is started, the ECS sends the SOR (start of run) command to all participating detectors. The same applies when a run ends for the command EOR (end of run) or when a run crashes. Therefore, in addition to the commands shown in Figure 4.3, the top node must be configured to be able to receive the SOR/EOR commands from the ECS not only in the READY state, but in all of its synchronous states, allowing FDD to participate in calibration, synthetic and technical runs. When the top node receives the ECS commands, it sends them to the FDD_DCS_RUN node, which is the one that actually reacts to those commands according to Figure 4.18. Initially, whenever the detector is not participating in a run, the FDD_DCS_RUN will be in RUN_OK state by default, regardless of the state of the top node. When a run is configured and the top node receives the SOR command, FDD_DCS_RUN goes to the SOR_PROGRESSING state and then back to the RUN_OK state when

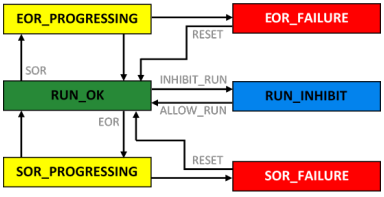

Figure 4.18: State diagram for FDD_DCS_RUN node.

the run actually starts. The same applies for the ending of a run with command EOR and the state EOR_PROGRESSING. If a run crashes while starting or ending, the node will move to the SOR_FAILURE or EOR_FAILURE states, and the RESET command can be issued to return to the RUN_OK state. A run can also be inhibited and allowed again.

Chapter 5

Operation of FDD DCS

5.1 Alarms

The alarm system is one of the most important features of the DCS that ensures the safe operation of our subdetector. The purpose of an alarm is to bring an anomalous situation to the attention of the operator[29]. This way, critical variations of parameters that might damage the equipment (such as PMTs voltage or current levels, or the electronic boards temperature) are promptly identified and appropriate actions can be taken. Alarms are displayed in a special panel (Figure 5.1) included in the JCOP Framework. In this panel the operator can see the datapoint related to the alarm, its value, the time of the event, a brief description, and a color-coded label according to its severity. Through this panel, alarms can be acknowledged to indicate that the case is being handled; and help files, with simple instructions for the operator to correct the issue, can be accessed.

Alarms are divided into three classes, according to the faulty datapoint value and the level of danger/error it represents for the system. These classes, and their corresponding colour, are described in Table 5.1.

Alarm class	Colour	Description
Warning	Yellow	Indicates a minor or a temporary anomaly, which can resolve itself or can progress into a more severe class. During data taking, DCS operators might not react to alarms belonging to the Warning class.
Error	Orange	This alarm class indicates a severe condition which does not represent imminent danger but shall be treated by the expert without delays.
Fatal	Red	This alarm class indicates an imminent danger and shall be treated by the operator or the expert immediately with higher priority.

Table 5.1: Alarm classes.

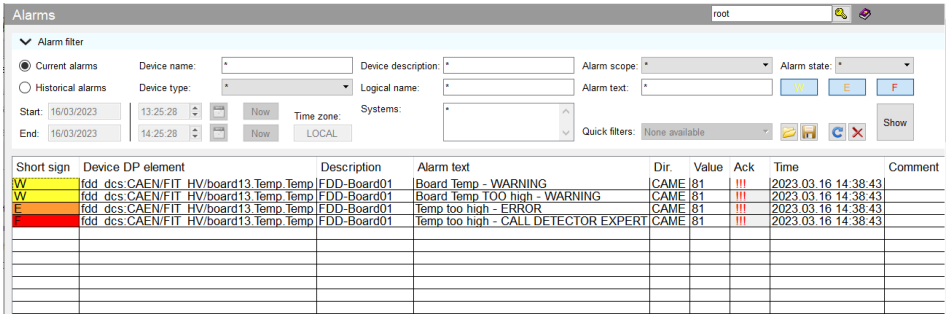

Figure 5.1: Alarm panel.

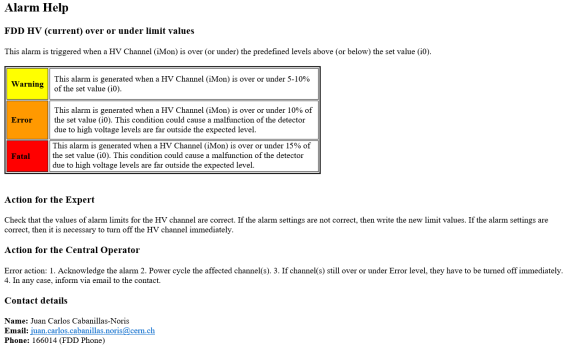

Alarm Help

FDD HV (current) over or under limit values

This alarm is triggered when a HV Channel (iMon) is over (or under) the predefined levels above (or below) the set value (i0).

Warning	This alarm is generated when a HV Channel (iMon) is over or under 5-10% of the set value (i0).
Error	This alarm is generated when a HV Channel (iMon) is over or under 10% of the set value (i0). This condition could cause a malfunction of the detector due to high voltage levels are far outside the expected level.
Fatal	This alarm is generated when a HV Channel (iMon) is over or under 15% of the set value (i0). This condition could cause a malfunction of the detector due to high voltage levels are far outside the expected level.

Action for the Expert

Check that the values of alarm limits for the HV channel are correct. If the alarm settings are not correct, then write the new limit values. If the alarm settings are correct, then it is necessary to turn off the HV channel immediately.

Action for the Central Operator

Error action: 1. Acknowledge the alarm 2. Power cycle the affected channel(s). 3. If channel(s) still over or under Error level, they have to be turned off immediately. 4. In any case, inform via email to the contact.

Contact details

Name: Juan Carlos Cabanillas-Noris
Email: juan.carlos.cabanillas.noris@cern.ch
Phone: 166014 (FDD Phone)

Figure 5.2: Alarm help file for out-of-range current values of the FDD PMTs

5.1.1 Alarm help

Every time an alarm appears, it must be handled according to its class. For this purpose, a help file must be associated with every alarm, meant to serve as a guide for the operator. These files are easily accessed from the central DCS console by right-clicking on the alarm line in the alarm panel. The files consist of a set of actions for the operator to take according to the severity of the alarm. The instructions should be short and understandable by non experts[29]. Figure 5.2 is an example of an alarm help file for alarms triggered by PMT current levels out of the desired range.

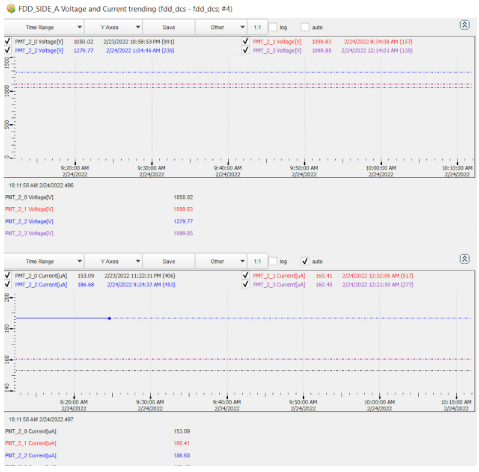

Figure 5.3: Trending plots for voltage and current levels of FDD-A.

5.2 Trending

The trending plots are another useful tool to permanently monitor variations in temperature, voltage and current levels, and can also be used to display the change of various parameters of interest such as background and trigger rates or magnetic field intensity. Operators and experts can visualize how these parameters evolve through time and, given the case, identify patterns or unusual behavior that could lead to a potential risk to the subdetector even before an alarm appears. Experts can also evaluate the performance of the detector, identifying and correcting inappropriate configurations for data taking (in FDD's case, for example, the quality of the trigger signals can be assessed and improved). Several panels at different branches of the FSM tree or the AliDCS UI include or allow the user to access these trending plots. Figure 5.3 shows an example of PMT voltage and current trending plots accessible from FDD_SIDE_A panel, and Figure 5.4 displays trending plots for the rate of the triggers (Vertex, Central, Semi-central, OrA, OrC) generated by the FDD FEE.

5.3 Archiving

Data acquired by the DCS is stored in DCS archiving system. Relevant datapoint elements were selected and configured to store its values in the ORACLE database, which is installed in the ALICE counting rooms and replicated to a service ac-

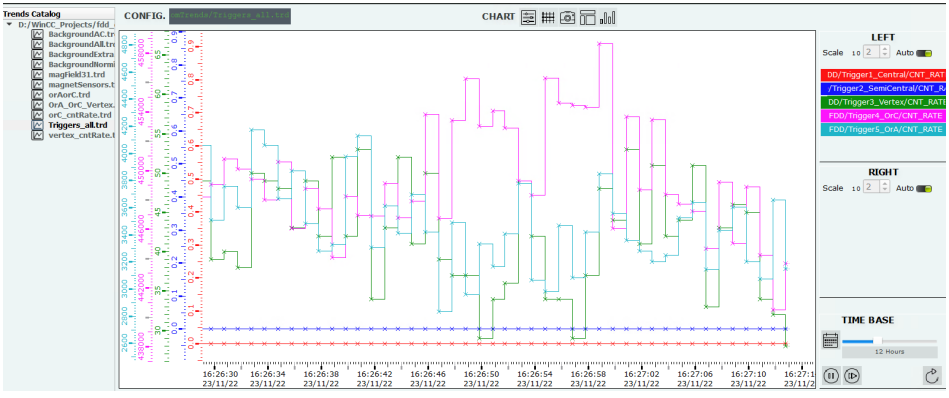

Figure 5.4: Trending plots for FDD-generated triggers rates.

cessible on CERN general network. The data includes operational parameters as well as data generated by the FEE including triggers, ADC baselines, PMT voltage and current. The stored data are available for later retrieval either directly from WINCC OA or by external clients. The DCS archive is primarily dedicated to long term data storage, to be used by detector experts for performance studies, etc. All trends use the DCS archive for retrieval and displaying of historical values. Some of these datapoints stored in ORACLE were also configured to be sent to ADAPOS (and further to the O2 system for online processing)[30]. After adding the archive settings, WINCC system starts streaming immediately to ADAPOS server, which transfers data to be streamed to O2. Then the offline experts configure the O2 side of the process, completing the chain.

5.4 Integration to ALICE

As it is explained in chapter 4, ALICE as a whole functions as a higher level FSM node for which all the detectors' FSMs are sub nodes of the same object type, consequently having the same available states and transitions. Furthermore, the state of ALICE depends on the state of its sub-nodes (the detectors). The same applies for the Safety Condition of ALICE, also dependent of the detectors' own Safety Condition. For this mechanism to work, all detectors must be integrated to the ALICE central DCS and the ALICE SAFE matrix. Detectors excluded from SAFE matrix do not contribute to ALICE SAFE state calculation and are not protected by the central DCS during the handshake procedure[31]. ALICE is controlled, operated and monitored by the crew in the ACR. In this room, the safety condition and the state of each detector is permanently visible in the DCS

monitor screen.

To fulfill the integration process to the central DCS, there is a series of requirements established by ALICE[28], including:

- Connection to ALICE's central systems, such as UI, ECS, FSM and SAFE; this allows for the detector to be operated centrally.
- Connection to and proper configuration of Alert system.
- Proper configuration of the detector's name and number, as well as WN alias.
- Proper definition of Safety operations such as GO SAFE, GO SUPERSAFE, RESTORE SAFE, etc. During integration tests, all of these operations are tested.
- Proper FSM configuration following ALICE convention for colours, keywords, available commands and states, etc.
- Implementation of a main user interface panel available for DCS operators.

5.5 SAFE operations

Regular operation of ALICE is related to the LHC beam life cycle[32], which roughly consists of the following steps: injection beam, ramp, flat top, squeeze, adjust, stable beams, beam dump and ramp down. Handshakes are mandatory at every corresponding critical transition injection, adjust and dump.

ALICE requires certain conditions for routine operation proceedings like handshake for inminent beam injection and beam dump, ALICE magnets ramp-up and ramp-down, ECS commands start-of-run and end-of-run, and other safety procedures (announced power cuts or electrical perturbation). Therefore, each time these operations take place, all detectors must change their states and/or conditions. From the operational point of view, detectors must be able to switch between a beam safe state and an operational state where data taking can start, reacting to a single command issued by the central DCS operator. A similar mechanism is implemented in case the detector is sensitive to magnetic field changes. When a ramp of solenoid or muon dipole is planned, a command is sent to all detectors and an immediate reaction is expected, in order to reach a global safe state. The safe conditions are set by detector's logic in a datapoint (EmergencyButton).

5.6 Automation process

In order to optimize the data taking process, the ALICE detectors have to reconfigure its devices (specially electronics and HV) and prepare them each time a run starts. This is particularly important because, for most detectors, proper configuration for data taking is lost during SAFE and/or MAGNET SAFE transitions. In FDD's case, HV configuration is lost when issuing GO SAFE command due to the fact that FDD is brought to BEAM_TUNING state and thus the PMTs voltage is set to zero. FEE configuration is lost with every GO DIPOLE/MAGNET SAFE because the Wiener crate is turned off. Furthermore, some detectors set different configurations for different types of runs, so they must be reconfigured when a new run type is set.

While manual configuration is possible to be performed by detector experts and/or DCS shifters (given the proper instructions), it is not at all the optimal procedure; it is virtually impossible for detector experts to be permanently monitoring their devices, and manual configuration always takes extra time to be carried out. Therefore, and automated configuration process is required.

To ensure that FDD will always be able to participate not only in regular data taking during collisions but also different types of runs such as technical, calibration and synthetic, a control manager script monitoring the commands sent by the central DCS to the FSM top node and the state of the top node itself was implemented in the WinCC OA project, and the automatic loading of proper HV recipes and Control Server configuration files was configured in this script; scripts controlling the SAFE and MAGNET SAFE transitions were also modified to implement recipe loading to cover all possible scenarios in which FDD loses HV and/or FEE configuration; For instance, receiving the GO READY command after a GO SAFE transition, which means FDD is in BEAM TUNING state (equivalent to SAFE condition), or receiving the GO STANDBY command after a GO MAGNET/DIPOLE SAFE transition, which means FDD is in OFF state (equivalent to MAGNET SAFE).

Both the FSM architecture and the Safety conditions for FIT (and thus FDD) were subject to several discussions and changes before and after the start of Run 3. Every time these configurations changed, the automated configuration procedure for FDD had to be adjusted accordingly.

5.7 FDD in Run 3

Once the FDD DCS was succesfully integrated to the ALICE DCS, it began participating in regular data taking for LHC Run 3 that started in July 2022. Figure 5.5 shows some FDD plots in the ALICE QC GUI obtained in Van der

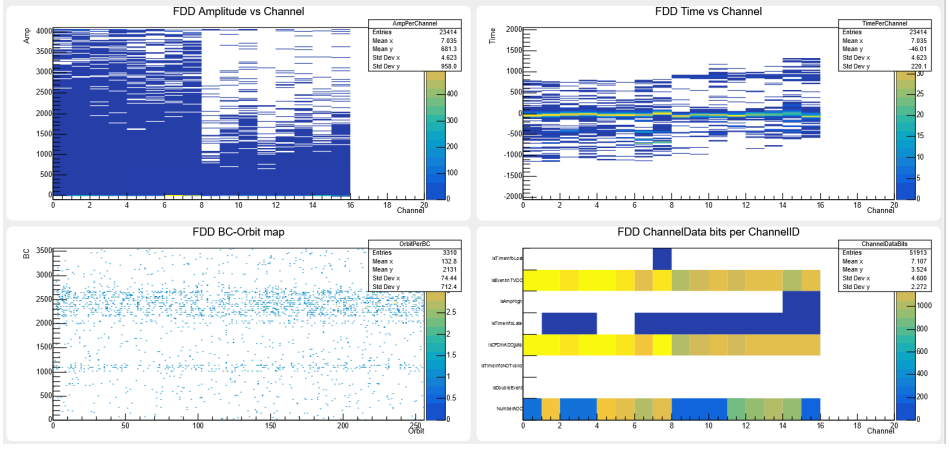

Figure 5.5: FDD plots for LHC Van der Meer luminosity scans.

Meer scans (LHC luminosity measurements) that took place in November 2022, and Figure 5.6 the plots obtained during the first lead ion collisions at record 5.36 TeV centre-of-mass energy per nucleon pair, also in November 2022.

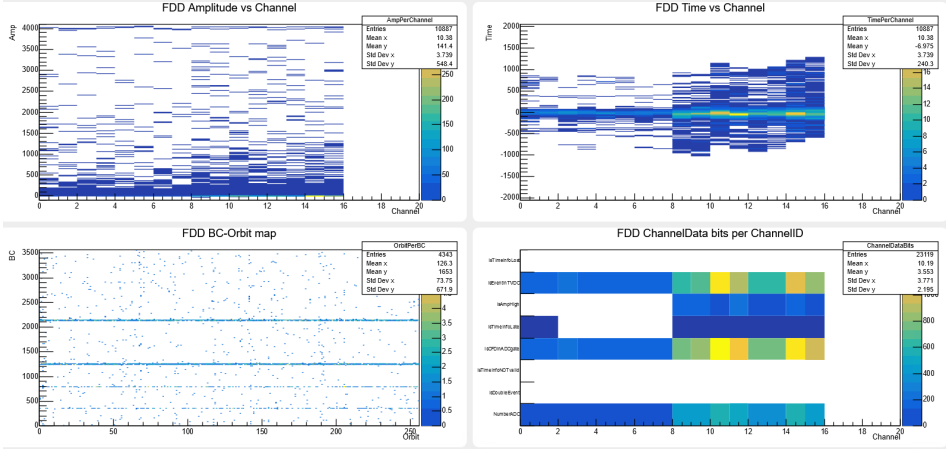

Figure 5.6: FDD plots for first Pb ion collisions of LHC Run 3.

Chapter 6

Conclusions

The Forward Diffractive Detector was successfully constructed, installed, commissioned, and integrated to the ALICE experiment between 2021 and 2022. The installation process required the addition of a new laser calibration system as well as connection to a new FEE. Calibration of FDD with this new systems was performed both before and after installation to obtain ideal operational parameters. These parameters were saved in high voltage and FEE recipes. The FDD DCS was developed according to the ALICE guidelines for regular operation, safety procedures, and data management. The FIT project standards including common panels, nodes, transitions and datapoints were also adapted to FDD's hardware architecture and its specific operation and safety requirements. Integration tests of the FDD DCS project with the high voltage and FEE hardware were succesfully performed at CERN, and the project was later installed in the FDD DCS Worker Node. The software and control architectures presented in this thesis provide an operative DCS for FDD that allows for safe operation, monitoring, visual displaying and automated configuration of the FDD hardware systems: high voltage, laser calibration and FEE. The configuration procedure that automatically loads high voltage and FEE recipes was implemented and optimized to ensure FDD readiness for any of the different LHC run types or physics studies to be performed. The DCS also allows for categorizing, monitoring, selecting, saving and sending to the ALICE database both the operational physics parameters and the FEE generated physics data. These data are later used for physics data reconstruction during data analysis. Based on these results, FDD is already participating in LHC Run 3 and provides level-zero triggers that are essential for the operation of several ALICE detectors. By the end of 2022, the detector has already successfully participated in data taking for Pb-Pb collisions tests, and has also contributed to luminosity measurements participating in van der Meer scans. FDD is expected to have an

important contribution in studies of ultra-peripheral collisions by extending the pseudorapidity coverage of ALICE. FDD-DCS has improved with respect to AD-DCS by integrating the new laser calibration and Control Server systems. The FDD-DCS system is fully operational and integrated into the Central DCS in the ALICE Run Control Center. The work presented in this thesis was the basis for the manuscript of the paper "Forward Diffractive Detector control system for Run 3 in the ALICE experiment"[21], which has already been published in the journal Nuclear Instruments and Methods in Physics Research A. Finally, the FDD DCS team is constantly improving, and adding new features and functionalities to the FDD-DCS with the aim of further optimizing the operation and data taking processes.

Bibliography

[1] L. Evans, P. Bryant, LHC Machine, Journal of Instrumentation 3 (2008) S08001.

[2] ALICE Collaboration, K. Aamodt, A.A. Quintana, R. Achenbach, S. Acounis, D. Adamová, et al., The ALICE experiment at the CERN LHC, Journal of Instrumentation 3 (2008) S08002.

https://doi.org/10.1088/1748-0221/3/08/s08002.

[3] M. Slupecki, The Fast Interaction Trigger for the ALICE Upgrade, PhD Thesis, University of Jyvaskyla, 2020. Available at: http://cds.cern.ch/record/2741462

[4] ALICE Collaboration, The ALICE experiment - A journey through QCD, CERN, 2022.

[5] ALICE Collaboration, Technical Design Report for the Upgrade of the Online-Offline Computing System, CERN-LHCC-2015-00. Avaliable at: https://cds.cern.ch/record/2011297/files/ALICE-TDR-019.pdf

[6] S. Rojas Torres for the ALICE collaboration, The Forward Diffractive Detector for ALICE, in: Proceedings of Science, The Eighth Annual Conference on Large Hadron Collider Physics-LHCP2020 25-30 May, 2020 online. Available at: https://pos.sissa.it/382/221/pdf.

[7] V. Zabloudil, Construction and comissioning of the FDD detector, Bachelor Thesis, Department of Physics, Faculty of Nuclear Sciences and Physical Engineering, Czech Technical University in Prague, 2021.

[8] S. Rojas Torres, The performance of ALICE-Diffractive detector in a beamtest, PhD Thesis, Universidad Autónoma de Sinaloa, México, 2018. Available at: http://cds.cern.ch/record/2657801

[9] Luminnotech - Luminophores.

Available at: https://www.luminnotech.com/products/luminophores (accessed July 18, 2022).

[10] Fast Timing BC-418, BC-420, BC-422, BC-422Q — Crystals. Available at: https://www.crystals.saint-gobain.com/radiation-detection-scintillators/plastic-scintillators/fast-timing-bc-418-bc-420-bc-422-bc-422q (accessed July 18, 2022).

[11] S. R. Klein, Ultra-peripheral collisions and hadronic structure, Nuclear Physics A 967 (2017), Pages 249-256.

https://doi.org/10.1016/j.nuclphysa.2017.05.098

[12] B. Abelev et al for the ALICE Collaboration, Upgrade of the ALICE Experiment: Letter Of Intent. J. Phys. G: Nucl. Part. Phys. 41 (2014) 087001.

[13] SIMATIC WinCC Open Architecture Portal (Internet).

Available at: https://www.winccoa.com/company.html (cited 2022 Jun 30).

[14] CERN. About JCOP (Internet). Available at: https://jcop.web.cern.ch (cited 2022 Oct 21).

[15] OPC Foundation (Internet). Available at: https://opcfoundation.org/about/what-is-opc/ (cited 2022 Oct 30).

[16] C. Gaspar et al, DIM (Internet). Available at: https://dim.web.cern.ch/ (cited 2022 Oct 30)

[17] C. Gaspar, JCOP Framework Hierarchical Controls Configuration Operation, 2004 (Internet). Available at: http://lhcb-online.web.cern.ch/ecs/fw/FSMConfig.pdf (accessed February 1, 2023)

[18] M. Tkáčik et al, FRED—Flexible Framework for Frontend Electronics Control in ALICE Experiment at CERN, Processes 8 (2020).

https://doi.org/10.3390/pr8050565

[19] P. Chochula et al., Challenges of the ALICE Detector Control System for the LHC Run3, in: 16th Int. Conf. on Accelerator and Large Experimental Control Systems, Barcelona, Spain, 2017. Available at: https://cds.cern.ch/record/2306220/files/tumpl09.pdf

[20] J. Lång et al. ADAPOS: An architecture for publishing ALICE DCS conditions data, in: 16th Int. Conf. on Accelerator and Large Experimental Control Systems, Barcelona, Spain, 2017. Available at: https://cds.cern.ch/record/2306223/files/tupha042.pdf

[21] J.M. Mejía Camacho, S.A. Rodríguez Ramírez et al, Forward Diffractive Detector control system for Run 3 in the ALICE experiment, Nuclear Inst. and Methods in Physics Research, A 1050 (2023) 168146.

[22] CAEN, SY4527 - Universal Multichannel Power Supply System, available at: https://www.caen.it/products/sy4527/ (accessed February 9, 2022).

[23] CAEN, A7030 - 12/24/36/48 Channel 3 kV/1 mA (1.5W) Common Floating Return Boards, available at: https://www.caen.it/products/a7030/ (accessed February 9, 2022).

[24] Photomultiplier tube assembly H8409-70 (Internet). Available at: https://www.hamamatsu.com/eu/en/product/type/H8409-70/index.html (Accesed March 15 2022).

[25] D. Finogeev, T. Karavicheva, D. Serebryakov, A. Tikhonov, W.H. Trzaska, N. Vozniuk, Readout system of the ALICE Fast Interaction Trigger, J. Inst., 15 (2020) C09005.

https://doi.org/10.1088/1748-0221/15/09/C09005

[26] D. Finogeev, on behalf of the ALICE collaboration, Fully integrated digital readout for the new Fast Interaction Trigger for the ALICE upgrade, Nuclear Inst. and Methods in Physics Research, A 952 (2020) 161920.

https://doi.org/10.1016/j.nima.2019.02.047

[27] G. De Cataldo, A. Augustinus, M. Boccioli, P. Chochula, L.S. Jirdén, Finite State Machines for Integration and Control in Alice, in: Proceedings of ICALEPCS07, Knoxville, Tennessee, USA, 2007, pp. 650–652. Available at: https://accelconf.web.cern.ch/ica07/PAPERS/RPPB21.PDF

[28] ALICE DCS 2021 Integration guidelines (Internet). Available at: https://espace.cern.ch/alicecontrols/DCSDocuments/Guidelines/Forms/AllItems.aspx (cited 2022 Nov 15).

[29] CERN, Guidelines for alarm setting, 2021.

Available at: https://espace.cern.ch/alicecontrols/DCSDocuments (Accessed February 20, 2022).

[30] P. Buncic, M. Krzewicki, P. Vande Vyvre, Technical Design Report for the Upgrade of the Online-Offline Computing System, CERN, Geneva, Switzerland, 2015. http://cds.cern.ch/record/2011297.

[31] The ALICE DCS operation manual, 2022 (Internet).

Available at: https://espace.cern.ch/alicecontrols/DCSDocuments (Accessed February 20, 2023).

[32] R. Alemany, M. Lamont and S. Page, Functional specification: Lhc modes. Technical Report LHC-OP-ES-0005 rev 1.5, CERN, 03 2015.